

Dynamic Scattering from Semiflexible Polymers

KLAUS KROY AND ERWIN FREY

1	Introduction	2
2	Wormlike chain model	5
3	Static structure factor	10
4	Critical comment on Gaussian models	12
5	Dynamics of semiflexible polymers in solution	15
5.1	Brief survey of the history	15
5.2	Introduction of the equation of motion	16
5.3	Linear mode analysis	20
5.4	Entanglement effects	23
6	Dynamic structure factor	28
6.1	Definitions	29
6.2	Initial decay ($t \ll \tau_q$)	30
6.3	Stretched exponential decay ($t \gg \tau_q$)	34
6.4	Entanglement effects	35
6.5	Polydispersity and clusters	37
6.6	Applications to biopolymers	39
7	Conclusions	41
A	Initial slope from the Smoluchowski equation	43
B	Glossary of symbols	45

*Book chapter in "Scattering in Polymeric and Colloidal Systems",
ed. by Wyn Brown and Kell Mortensen,
Gordon and Breach*

Final version of July 3, 2001

1 Introduction

Semiflexible polymers are macromolecules with a stiffness intermediate between the two extreme cases of random coils and rigid rods. The stiffness is conveniently characterized by the *persistence length* ℓ_p , which is defined as the arc length or ‘chemical distance’, over which the tangential correlations of the contour decay to $1/e$. Only if this length is much smaller than the total contour length L and the typical length scale of observation λ , can the polymer be regarded as a flexible chain (of Kuhn length $2\ell_p$) and can be described by the standard models for flexible polymers [21]. For many naturally occurring polymers ℓ_p is *not* very small with respect to L or λ or both of them, so that the flexible chain models are not appropriate. On the other hand, molecular self-interactions, which complicate substantially the mathematical modeling for molecules with a total contour length more than hundred times larger than ℓ_p , can safely be neglected. Especially some thread-like biomolecules such as actin filaments, intermediate filaments, microtubuli, DNA, collagen etc., which play an important role in cell biology [78, 44, 50], are good examples of what physicists have in mind when they think of semiflexible polymers. Some of these molecules have persistence lengths that are by several orders of magnitude larger than their lateral diameter and are comparable to or even longer than their contour length. In many cases their huge dimensions (L can be of the order of several micrometers) render their internal dynamics accessible to light scattering techniques and even to light microscopy. (To give the reader an impression of a typical experimental system, we have reproduced in Fig. 1 an electron micrograph of a semidilute actin solution from Ref. [33].) Certain cylindrical assemblies of amphiphilic molecules, so called wormlike micelles, can also be regarded as semiflexible chains. And there is, of course, a variety of synthetic polymers to which the notion of semiflexibility applies. We will argue below that the failure of the common flexible chain models for semiflexible macromolecules becomes especially apparent in their dynamical properties. This is a consequence of the hydrodynamic interaction, which obeys a reciprocal distance law, giving strong weight to the small scale structure.

Historically, much work has been devoted to the analysis of what we call *Gaussian models*. These are rather direct extensions of the well known Gaussian chain model for a flexible polymer. One of the first dynamic theories of that kind was that by Harris and Hearst [39]. It was criticized for its intrinsic inconsistencies by many authors [86, 5, 97]. In fact, even the latest descen-

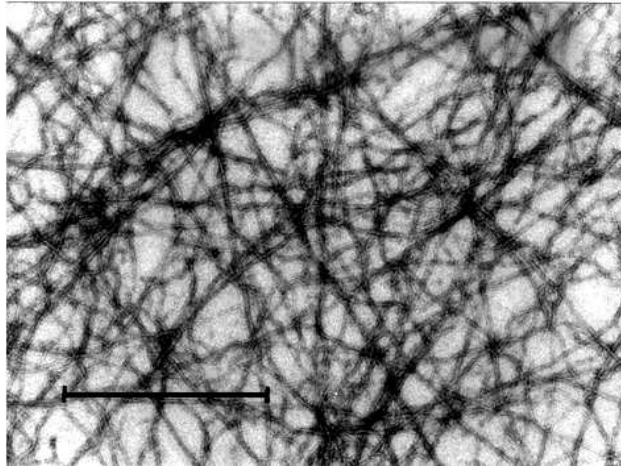


Figure 1: Electron micrograph of a 0.4 mg/ml actin solution polymerized in vitro [33]. The bar indicates the length of 1 μm .

dants of this theory predict a Gaussian distribution function centered at zero [97] for the spatial distances of contour elements separated by a chemical distance s . This becomes invalid (even qualitatively) for arc lengths s shorter than the persistence length, as the reader may convince him/herself by comparing this function to the δ -function located at s which it should approach in the limit $s/\ell_p \rightarrow 0$ [96]. In view of this severe fundamental shortcoming of the Gaussian models, we suggest that starting from the Gaussian chain for modeling semiflexible polymers means to ‘put the cart before the horse’, and that a stiff rod might be a more natural starting point. Indeed, it is the opinion of the authors (supported by experimental evidence) that the model of a *weakly bending rod* not only captures the essential properties of semiflexible polymers, but can also serve as a useful quantitative description in a number of practical applications. More specifically, for most of the following we restrict the discussion to the ideal case that the *scattering wavelength* λ is shorter than both the persistence length and the contour length of the polymers. In this case the theoretical results are simple analytic expressions and thus readily applied. Moreover, the number of phenomenological parameters can be kept small, which also facilitates quantitative comparison with experiment (e.g. to determine the lateral diameter or the bending stiffness of the polymer by dynamic light scattering).

We start this contribution with a pedagogical review of our current un-

derstanding of the *wormlike chain model*, which is the ‘minimal model’ of a semiflexible polymer. This model has been very successful in describing various aspects of single semiflexible polymers such as their extension under applied external forces [85]. The importance of the local rigid constraint of constant contour length is emphasized, and the fundamental differences to the well known Gaussian chain are discussed. After a brief review of some work concerned with the calculation of the static structure factor we give a detailed derivation of the intermediate scattering function for a weakly bending wormlike chain in solution. Two different scaling regimes are discernible for which simple asymptotic expressions are found. For short times the motion is dominated by the hydrodynamics of the solvent and the structure factor is expressed as a simple exponential. For long times the conformational relaxation due to the wormlike chain Hamiltonian leads to a stretched exponential tail. Which of the two regimes dominates the decay of the scattering function depends on the product $q\ell_p$ of the *scattering wave vector*¹ $q \equiv 2\pi/\lambda$ and the persistence length ℓ_p . In contrast to the Rouse and Zimm models, where the stretched exponential regime is not reached before several characteristic decay times (where the dynamic structure factor has practically decayed to zero) [2, 35, 42], the stretched exponential tail dominates for semiflexible chains with $q\ell_p \gg 1$. This is a consequence of the existence of two characteristic time scales rather than one, which in turn is due to the existence of the additional length scale ℓ_p . Since the initial decay rate is not a universal number as in the Zimm model, but depends on the diameter of the chain backbone, also the initial decay regime itself contains some valuable information about the polymer. This result can be regarded as an extension of the particle sizing method to the case of polymers with $L \gg \lambda$. To put it as a pointed provocation: while the dynamic structure factor calculated from the standard flexible polymer models is essentially a Lorentzian of universal width, the semiflexible case is substantially richer.

In semidilute solutions the fluctuations of a test polymer are restricted by the surrounding polymers, which act as a tube-like cage that slows down the decay of correlations for long times. We discuss extensions of the theory for a single semiflexible polymer to include the main effects from interactions with the surrounding medium, which by itself is subject to thermal fluctuations.

¹For a light scattering experiment $q \equiv 4\pi n/\lambda_0 \cdot \sin(\theta/2)$, with n , λ_0 and θ denoting the index of refraction of the medium, the vacuum wavelength of the light source, and the scattering angle, respectively.

We also add some general remarks on polydispersity, clusters and aggregation and mention applications of the theory to experimental data.

2 Wormlike chain model

The statistical mechanics of a semiflexible polymer is already by itself a very interesting and nontrivial problem with quite a number of recent developments 50 years after it was first formulated by Kratky and Porod [54]. Since we are mainly interested in the dynamics we will be brief in our discussion of the static properties restricting ourselves to those features which are most important for dynamics. For a more detailed analysis we refer the reader to some recent review articles [25, 24].

The theoretical minimal model of a semiflexible polymer is the continuous version² of the Kratky-Porod chain also known as *wormlike chain model* [79], where the polymer is represented by a differentiable space curve $\mathbf{r}(s)$ of contour length L .

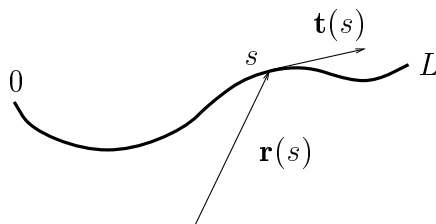


Figure 2: Sketch of the wormlike chain as a differentiable space curve $\mathbf{r}(s)$ of contour length L parameterized by arc length s . Also indicated is the tangent vector $\mathbf{t}(s)$.

Its statistical properties are determined by a free energy functional (the “Hamiltonian”)

$$\mathcal{H} = \frac{\kappa}{2} \int_0^L ds \left(\frac{\partial^2 \mathbf{r}(s)}{\partial s^2} \right)^2 \quad (1)$$

which measures the total elastic energy of a particular conformation by the integral over the square of the local curvature weighted by the *bending modulus* κ of the chain. To ensure that the second derivative in the integrand is really the curvature of the chain, we have to enforce the parameter s to be arc length. For a virtually inextensible backbone we thus have to impose

²The discrete version is equivalent to a one dimensional classical Heisenberg chain [23, 92].

the *local rigid constraint* $|\mathbf{t}(s)| = 1$ on the tangent vector $\mathbf{t}(s) = \partial\mathbf{r}/\partial s$. We will see that this constraint is indeed essential for a correct description of the static as well as the dynamic properties of semiflexible polymers. On the other hand, it presents a considerable mathematical difficulty for the calculation of statistical properties of the model.

Due to these mathematical complications, which are the same as for a classical Heisenberg chain, only few of the statistical properties of the worm-like chain can be extracted analytically, the best known being

- the exponential decay of the tangent-tangent correlation function

$$\langle \mathbf{t}(s)\mathbf{t}(s') \rangle = \exp(-|s - s'|/\ell_p), \quad (2)$$

with the persistence length $\ell_p = \kappa/k_B T$ (in three dimensional embedding space),

- the mean-square end-to-end distance [54]

$$\mathcal{R}^2 := \langle [\mathbf{r}(L) - \mathbf{r}(0)]^2 \rangle = L^2 f_D(L/\ell_p), \quad (3)$$

- and the radius of gyration [8]

$$\begin{aligned} \mathcal{R}_g^2 &:= \frac{1}{2L^2} \int_0^L ds \int_0^L ds' \langle [\mathbf{r}(s) - \mathbf{r}(s')]^2 \rangle \\ &= \ell_p^2 (f_D(L/\ell_p) - 1 + L/3\ell_p). \end{aligned} \quad (4)$$

For notational convenience we have introduced the function

$$f_D(x) = 2(e^{-x} - 1 + x)/x^2. \quad (5)$$

For extreme ratios of L/ℓ_p Eq. (2) – (4) reduce to the appropriate limits of a flexible chain with a statistical segment length (or Kuhn length) $2\ell_p$ and a rigid rod, respectively,³

$$\mathcal{R}^2 = \begin{cases} L^2 & (L \ll \ell_p) \\ 2\ell_p L & (L \gg \ell_p) \end{cases}, \quad \mathcal{R}_g^2 = \begin{cases} L^2/12 & (L \ll \ell_p) \\ 2\ell_p L/6 & (L \gg \ell_p) \end{cases}. \quad (6)$$

³As a side remark we note that the reasonable behavior of the second moments by itself is not at all a sufficient condition for a model to be regarded as a satisfying description of a semiflexible polymer (cf. Section 4).

The calculation of higher moments becomes increasingly troublesome [40]. For later use, we also want to mention a property of the wormlike chain model that immediately can be read off from the Hamiltonian by dimensional analysis. For a stiff wormlike chain ($\ell_p \gg L$) the length fluctuations of the end-to-end distance are only of second order in the amplitudes of the transverse fluctuations. In the Monge representation the fluctuations of the end-to-end vector of the chain can therefore be described in purely transverse coordinates \mathbf{R}_\perp , and the rigid constraint is fulfilled automatically. It is then easy to see that the amplitude R_\perp of transverse undulations of the end-to-end vector $\mathbf{R} \equiv \mathbf{r}(L) - \mathbf{r}(0)$ scales as

$$R_\perp^2 \propto L^3/\ell_p \quad (7)$$

with the contour length L . Since this property does not depend on L being the total contour length but holds for arbitrary subsections of the contour, this implies that the contour of a weakly bending wormlike chain is *self-affine*, $R_\perp \propto L^\chi$ with a roughness exponent $\chi = 3/2$. It is this self-affine property which gives rise to static and dynamic scaling results for semiflexible polymers. In this respect it plays a role comparable to the fractal structure of the Gaussian chain for flexible polymers.

The function which contains the most comprehensive information about the statistical properties of the chain is the *probability distribution of the end-to-end vector*

$$G(\mathbf{r}; L) = \langle \delta(\mathbf{r} - \mathbf{R}) \rangle . \quad (8)$$

For a *freely jointed phantom chain* (a chain of freely hinged segments without self-interaction) this function is known exactly [98]. As for any model with short-ranged interactions it converges quickly to a Gaussian distribution

$$G_0(\mathbf{r}; L) = \left(\frac{3}{4\pi\ell_p L} \right)^{3/2} \exp\left(-\frac{3r^2}{4\ell_p L} \right) \quad (9)$$

for increasing number of segments. This is a consequence of the central limit theorem. For chains that are at least some $10\ell_p$ long the Gaussian can serve as an excellent approximation to $G(\mathbf{r}; L)$ for many purposes. For the freely jointed chain and also for the so called *freely rotating chain*⁴, the persistence length ℓ_p is independent of temperature because its microscopic

⁴In the freely rotating chain adjacent segments can rotate freely on a cone of fixed angle.

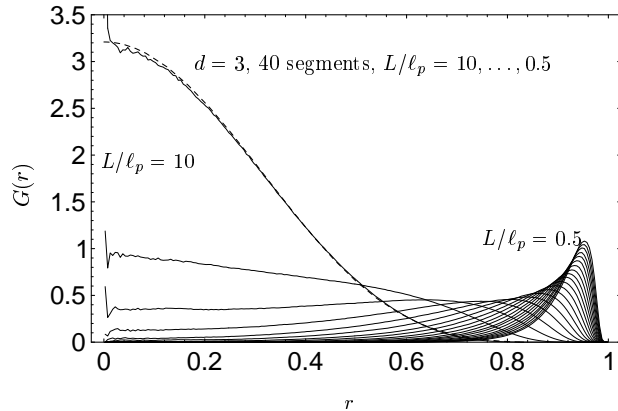


Figure 3: Numerical results for the end-to-end distribution function of a (discrete) wormlike chain in $d = 3$ dimensional space after Reference [96] without phase space measure $4\pi r^2$ (kindly provided by J. Wilhelm). Note that with increasing stiffness of the polymer there is a pronounced crossover from a Gaussian to a completely non-Gaussian form with the weight of the distribution shifting towards full stretching. The dashed line indicates the first Daniels approximation obtained by a perturbative approach around the Gaussian chain limit [16].

origin lies in steric constraints rather than in the bending stiffness of the backbone as suggested by the wormlike chain Hamiltonian Eq. (1). This difference is sometimes emphasized by introducing the Kuhn length $b = 2\ell_p$ as a material parameter in place of the bending modulus κ . The well known minimal model of a flexible polymer, the (continuous) *Gaussian chain*, is obtained by demanding Eq. (9) to hold down to arbitrarily short length scales⁵. Corrections to Eq. (9) to account for a finite (but small) persistence length of a semiflexible chain have been worked out by Daniels [16] (see Fig. 3).

For a Gaussian chain, the separation by a given distance r of any two segments with preferred mean-square distance $2\ell_p s$ is punished by the free energy cost $F(\mathbf{r}) = -k_B T \ln G_0(\mathbf{r}; s) = \text{const.} + 3k_B T \mathbf{r}^2 / 4\ell_p s$ and therefore requires a force

$$\mathbf{f} = \frac{\partial F}{\partial \mathbf{r}} = \frac{3k_B T}{2\ell_p s} \mathbf{r}. \quad (10)$$

⁵This innocent looking prescription is actually a renormalization that defines a fractal object. The *physical* contour parameter s is defined with respect to the reference length ℓ_p . But only the product $\ell_p s$ of both lengths retains its physical meaning upon renormalization (i.e. in the limit $\ell_p \rightarrow 0$).

If ℓ_p is a temperature independent material parameter the restoring force is proportional to $k_B T$, which reveals the purely entropic nature of the conformational statistics of a freely jointed (or freely rotating) chain. The linear force extension relation can actually be evaluated exactly for a wormlike chain of arbitrary stiffness [55]. The result reproduces Eq. (10) in the flexible limit, but exhibits a strong dependence on the angle between the applied force and the average molecule axis in the rod limit. Transverse forces lead to ordinary mechanical bending, while the longitudinal spring coefficient diverges in the mechanical limit $T \rightarrow 0$ as $1/T$ for temperature independent κ . This vanishing of linear response is a remainder of the *Euler buckling instability* of rod mechanics. The latter also governs the end-to-end distribution of a wormlike chain in the weakly bending rod limit.

The characteristic feature of the physics of beam buckling is that the energy E_{cl} of a straight rod of length L and bending modulus κ is an almost linear function of its end-to-end distance R ,

$$E_{\text{cl}} \approx f_c \cdot (L - R). \quad (11)$$

Here $f_c = \kappa\pi^2/L^2$ is the critical force for the onset of the Euler instability. Neglecting fluctuations around the classical contour this would lead to an end-to-end distribution function with maximum weight at $R = L$,

$$G(\mathbf{r}; L) \propto \exp[-f_c \cdot (L - r)/k_B T]. \quad (12)$$

Note that with such an approach we completely ignore entropic effects which are the only contributions in case of the freely jointed chain, discussed above. In order to correct for this omission we have to multiply the Boltzmann weight in Eq. (12) by the relative number of allowed conformations. This becomes most obvious for a completely stretched chain, where up to global rotations only one possible configuration exists and consequently the end-to-end distribution function has to vanish.

Within a quantitative analysis of the wormlike chain Hamiltonian in Eq. (1) one can show that the end-to-end distribution function near the rod limit is given to a good approximation by [96]

$$G(\mathbf{r}; L) \approx \frac{\ell_p}{\mathcal{N}L^2} F\left(\frac{\ell_p}{L}(1 - r/L)\right), \quad (13)$$

with

$$F(x) = \begin{cases} \frac{\pi}{2} \exp[-\pi^2 x] & \text{for } x > 0.2 \\ \frac{1/x - 2}{8\pi^{3/2} x^{3/2}} \exp\left[-\frac{1}{4x}\right] & \text{for } x \leq 0.2 \end{cases}$$

and \mathcal{N} a normalization factor close to 1. This result is valid for $L \lesssim 2\ell_p$, $x \lesssim 0.5$. The first expression for $F(x)$ is indeed equal to Eq. (12), while the second expression for stretched conformations is dominated by the entropic contributions, which guarantee the vanishing of $G(\mathbf{r}; L)$ at full extension. As can be seen in Fig. 3, the maximum weight of the distribution shifts towards full stretching as the stiffness of the chain is increased to finally approach a sharp peak at $R = L$ for the rigid rod.

3 Static structure factor

Static light scattering has been used in the past as a very convenient experimental tool to determine molecular parameters such as radii of gyration, molecular weights, and virial coefficients [30]. Persistence lengths have been determined for gelatin [73], polysaccharides, mesogenic polymers [12] and polystyrene [14], just to mention some examples. Interpolating formulas for the static structure factor [54, 53, 51] have been used extensively to extract model parameters from experimental data (see e.g. [41] and references therein). Numerical work by Yamakawa and coworkers [99, 100] and Monte Carlo data [72] are sometimes considered as a more precise reference.

The static structure factor or scattering function of a single chain is defined as the average sum of coherent scattering from any two points \mathbf{r}_n and \mathbf{r}_m along the chain

$$S(\mathbf{q}) = \frac{1}{N} \sum_{n,m}^N \langle \exp[i\mathbf{q} \cdot (\mathbf{r}_n - \mathbf{r}_m)] \rangle. \quad (14)$$

The wave vector dependence of the structure factor reflects the conformational statistics of the chain and (in the continuum limit) is related to the end-to-end vector distribution function $G(\mathbf{r}; s)$ through

$$S(\mathbf{q}) = \int_0^L ds (L - s) \int d^3r e^{i\mathbf{q} \cdot \mathbf{r}} G(\mathbf{r}; s). \quad (15)$$

Several limiting cases can be treated exactly. First, in the limit of small $q\mathcal{R}_g$ (Guinier range), when the scattering wavelength λ is large compared to the extension of the scattering object, one can expand Eq. (14)

$$\begin{aligned} S(\mathbf{q}) &= \frac{1}{N} \sum_{n,m}^N \langle 1 - q^2(\mathbf{r}_n - \mathbf{r}_m)^2/6 + \dots \rangle \\ &= N(1 - q^2\mathcal{R}_g^2/3 + \dots). \end{aligned} \quad (16)$$

The radius of gyration $\mathcal{R}_g^2 = (1/2N^2) \sum_{n,m}^N \langle (\mathbf{r}_n - \mathbf{r}_m)^2 \rangle$ introduced in Eq. (4) naturally appears as the first moment in this series expansion and can thus directly be determined from the small q region of the structure factor. The expansion can be (and has been) pushed to higher orders if higher moments $(\mathbf{r}_n - \mathbf{r}_m)^n$ can be calculated for a particular model. As we noted above, this becomes laborious for the wormlike chain model.

For the special case of rather long chains ($L \gtrsim 20\ell_p$) but still negligible self-interaction of the polymer, Sharp and Bloomfield [84] have calculated a formula for the scattering function $S(q)$ of a wormlike chain valid up to $q\ell_p \approx 1$ based on the first Daniels approximation [16] to the radial distribution function mentioned above. In the zeroth order approximation it reduces to the scattering function of a Gaussian chain calculated by Debye, which is given by the function $f_D(x)$ introduced in Eq. (5). The full expression is

$$S(x) = f_D(x) + \frac{2\ell_p}{15L} \left[4 + \frac{7}{x} - \left(11 + \frac{7}{x} \right) e^{-x} \right], \quad (17)$$

where $x = q^2 L \ell_p / 3$.

Exact expressions for $S(q)$ are also known in the infinite length limit $qL \rightarrow \infty$ and in the rigid rod limit $L/\ell_p \rightarrow 0$. In the latter case the scattering function approaches that of a rod [67],

$$S(q) = \frac{2N}{(qL)^2} [\cos(qL) - 1 + qL \text{Si}(qL)] \xrightarrow{qL \gg 1} \frac{\pi}{qa} - \frac{2}{q^2 a L} \quad (\text{rigid rod}). \quad (18)$$

Here, $\text{Si}(y)$ denotes the sine-integral $\int_0^y dx \frac{\sin x}{x}$. On the other hand, des Cloizeaux [19] has worked out the static structure factor for an infinitely long wormlike chain. For large scattering vectors, the leading correction to the rod asymptotics π/qa is $+2/3q^2 a \ell_p$. Later, the asymptotic behavior of $S(q)$ for stiff wormlike chains was obtained in a series expansion up to fifth order in L/ℓ_p [70], which reduces for large q to a combination of these results,

$$S(q) \xrightarrow{qL \gg 1} \frac{\pi}{qa} - \frac{2}{q^2 a L} + \frac{2}{3q^2 a \ell_p} \quad (\text{weakly bending rod}), \quad (19)$$

in accord with an earlier asymptotic analysis [53].

Finally, if a large intermediate regime $\ell_p \ll \lambda \ll \mathcal{R}_g$ is present, the intermediate behavior of the static structure factor can be estimated by a scaling argument. Generalizing the result for the Gaussian chain and Eq. (16), the

scaling form $S(q\mathcal{R}_g) =: Ns(q\mathcal{R}_g)$ with $s(0) = 1$ is assumed. The dependence on the scaling variable $q\mathcal{R}_g$ is determined by the condition that the scattering function becomes a power law in q independent of chain length N for large q ,

$$S(q) \propto N(q\mathcal{R}_g)^{-1/\nu} \propto q^{-1/\nu} \quad (\text{with } \mathcal{R}_g \propto N^\nu). \quad (20)$$

The argument amounts to idealizing the polymer as a self similar object of fractal dimension $1/\nu$ on intermediate scales, which (though not exact) has become a commonly adopted view for many applications [17]. Of course, any ideal self similar objects such as the infinite rigid rod ($\nu = 1$) or the infinite Gaussian chain ($\nu = 1/2$) obey Eq. (20) exactly. In general ν is a complicated function of the molecular interaction of the polymer with itself and the solvent.

The lack of a simple general formula for the structure factor of a polymer of arbitrary length and stiffness has also stimulated many authors to look for a convenient interpolation [54, 53, 51, 58, 59, 97, 62] between the exactly known cases of the rigid rod and the Gaussian chain. These interpolations are obtained by more or less convincing *ad hoc* approximation schemes. In the next section we briefly comment on a particular scheme that has also been applied to dynamics.

4 Critical comment on Gaussian models

One of the first attempts to find an interpolation formula for the static structure factor of a wormlike chain is due to Kratky and Porod, who for the first time introduced this model and calculated the second moment of the end-to-end vector, Eq. (3). This was a prerequisite for their calculation of the static structure factor, for which they proposed the prescription

$$\langle e^{i\mathbf{q}\mathbf{R}} \rangle \rightarrow e^{-\frac{1}{2}\langle \mathbf{q}\mathbf{R} \rangle^2} = e^{-q^2 \mathcal{R}^2/6} \quad (21)$$

as a ‘good approximation’ – despite the manifestly non-Gaussian character of their model at short length scales. This simple scheme gives indeed a reasonable first approximation to the static structure factor. (A discussion of the quality of different interpolations for the structure factor is beyond the scope of this contribution.) However, we want to dwell on a principle failure of Gaussian approximations to the wormlike chain. This is most dramatically seen in the end-to-end distribution function $G(\mathbf{r})$ defined in Eq. (8), which is directly related to the structure factor by Eq. (15). Introducing the Fourier

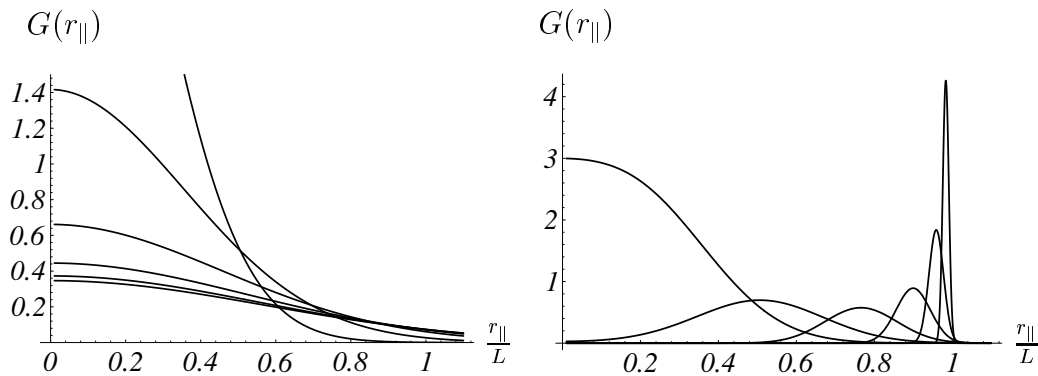


Figure 4: Failure of the Gaussian models (left) to reproduce the radial distribution function of a wormlike chain. Substantial improvement is attained with a simple trick (right), which demonstrates the crucial role of contour length fluctuations for the statistical properties of the model. The functions (without the factor $4\pi r^2$) have been plotted for logarithmically spaced ratios $\ell_p/L = 0.1 \dots 10$. For better comparison the length of the clamped wormlike chain has been renormalized so that $\langle R_{\parallel}^2 \rangle = \mathcal{R}^2$ of the free wormlike chain. See also the exact numerical data of Wilhelm and Frey [96] in Fig. 2.

representation of the δ -function into the definition and applying Eq. (21) we obtain, of course, a Gaussian distribution function

$$G(r) = (3/2\pi\mathcal{R}^2)^{3/2} \exp(-3r^2/2\mathcal{R}^2) . \quad (22)$$

This is plotted for various ratios L/ℓ_p in Fig. 4 (left).

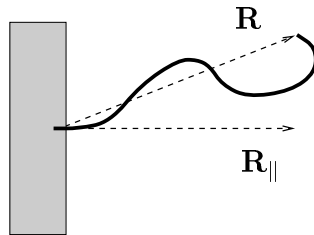


Figure 5: A grafted wormlike chain and the projection \mathbf{R}_{\parallel} of the end-to-end vector \mathbf{R} onto the direction of the clamped end.

It should be intuitively clear that this is a crude approximation to physical reality, because it replaces by a Gaussian centered at $r = 0$ a function that approaches a “delta-like” peak at $r = L$ in the stiff limit $\ell_p/L \rightarrow \infty$. Only

recently it has become more widely appreciated that approximations which neglect or soften too much the rigid constraint of constant tangent length in the wormlike chain model fail completely in describing the essential features of semiflexible polymers. Nevertheless, some ‘improved’ Gaussian models, which reproduce Eq. (22) identically, can be found in the literature [58, 59, 97, 62]. The problem persists in dynamic calculations, where the same sort of models (which may be characterized as ‘improved Harris-Hearst models’) have been analyzed extensively [36, 37, 38]. Without really going into the problem of an honest calculation of the radial distribution function [96], we want to give the reader a hint to the problem with Gaussian models by a simple argument for improving the Gaussian radial distribution function of Eq. (22). Without additional work we nevertheless can expect to get a result that is much more realistic than Eq. (22) (at least qualitatively), if we start from the observation that the distribution function will be peaked (if it is peaked at all) near $\langle \mathbf{R} \rangle$ rather than at zero. To circumvent the problem of the rotational isotropy of a free polymer chain, let us consider instead of \mathbf{R} the projection \mathbf{R}_{\parallel} of the end-to-end vector of a grafted wormlike chain onto the direction of the clamped end. Introducing the Fourier representation of the δ -function, we rewrite Eq. (8) as

$$G(\mathbf{r}_{\parallel}) = \int \frac{d^3 k}{(2\pi)^3} e^{i\mathbf{k}(\mathbf{r}_{\parallel} - \langle \mathbf{R}_{\parallel} \rangle)} \langle e^{i\mathbf{k}(\langle \mathbf{R}_{\parallel} \rangle - \mathbf{R}_{\parallel})} \rangle \quad (23)$$

and use the prescription Eq. (21) for deviations of the (projected) end-to-end distance \mathbf{R}_{\parallel} from its average $\langle \mathbf{R}_{\parallel} \rangle$. Evaluating the integral we obtain

$$G(r_{\parallel}) = \mathcal{N} r_{\parallel}^{-1} \sinh(3\langle R_{\parallel} \rangle r_{\parallel} / \rho^2) e^{-3r_{\parallel}^2 / 2\rho^2} \quad (24)$$

with \mathcal{N} a normalization constant and $\rho^2 = \langle R_{\parallel}^2 \rangle - \langle R_{\parallel} \rangle^2$. The problem thus again has been reduced to the calculation of low moments, namely $\langle R_{\parallel}^2 \rangle$ and $\langle R_{\parallel} \rangle$, which can easily be done for the wormlike chain [79, 55],

$$\langle R_{\parallel} \rangle = \ell_p (1 - e^{-L/\ell_p}) , \quad \langle R_{\parallel}^2 \rangle = \frac{2\ell_p^2}{9} \left(\frac{3L}{\ell_p} + e^{-3L/\ell_p} - 1 \right) . \quad (25)$$

The result is also plotted for several ratios ℓ_p/L in Fig. 4 (right) for comparison. Though this simple trick does not really give quantitatively useful results (compare to the exact numerical data [96] in Fig. 2), the curves in Fig. 4 give a qualitative impression of the most salient features of the radial

distribution function of a semiflexible polymer. Of course, due to the simplistic Gaussian scheme of Eq. (21) they still cannot reproduce the actual asymmetry of the peak and the essential singularity of $G(r)$ at $r = L$. But their derivation demonstrates the drastic influence of contour length fluctuations onto the statistical properties of the model. For a better approximation [10] to the radial distribution function and an exact solution in the weakly bending rod limit [96] we refer the curious reader to the literature.

5 Dynamics of semiflexible polymers in solution

5.1 *Brief survey of the history*

The dynamic properties of flexible polymers [21] are most simply described in terms of the famous “bead and spring” model originally proposed by Rouse [76]. However, the relation of this model to physical reality is loose. The Rouse model is motivated mainly by the success of the Gaussian chain model as a qualitative basic model for the static statistical properties of flexible polymers. Similar as the Gaussian chain in statics, it can be regarded as the minimal *dynamic* model of an ideal flexible polymer in the spirit of the renormalization group (i.e., in the limit $L/\ell_p \rightarrow \infty$ neglecting hydrodynamic interaction and self-interactions). It is obtained by equating the entropic spring-force of Eq. (10) – in the continuum limit – to the friction of a bead of the dimension of a statistical segment. There is no direct interpretation of the effective variables of ‘bead’ and ‘spring’ in terms of molecular parameters of the polymer, in particular in presence of long-ranged hydrodynamic and steric self-interactions. Nevertheless, the Rouse model and a refined version including hydrodynamic backflow effects, which was introduced by Zimm [102], have been applied with some success to interpret experimental data. In the case of semiflexible polymers we are in the fortunate situation that we can (and must, unfortunately) start from a more realistic description of the statics and dynamics. As for statics, the minimal model for the theoretical modeling is the wormlike chain introduced in Section 2. (We do not consider helical [101] and circular [87] wormlike chain models.) The difficulties of this model, which are mainly a consequence of the rigid constraint of constant tangent length, persist in dynamics. There is additionally the problem of hydrodynamic interactions. The temptation to simplify the model is therefore even larger in dynamics than in statics. From our experience with statics we expect the model to be most tractable in the limiting cases of rather flexible polymers or in the rigid rod limit, respectively. In the following we

will pursue the latter route. Of course, as in statics, there is a variety of possibilities to introduce interpolating models between the Gaussian chain and the weakly bending rod. The most common model of that kind is obtained by the attempt to account by a Lagrange multiplier [39] (or two of them [58, 59, 36, 37, 38]) for the rigid constraint of constant contour length, i.e. by the ‘Gaussian approximation’. There is, however, no reason why the fundamental shortcomings of Gaussian approximations, demonstrated in Section 4, should cease to persist in dynamic calculations and we will not discuss these models further. (In fact, a whole Lagrange multiplier *function* would be needed to enforce the rigid constraint properly [32, 83].) For a critical discussion of the pioneering work by Harris and Hearst [39], Saito *et al.* [79], and Fujime [27] the interested reader may consult the article by Soda [86]. The latter also contains a derivation of the equation of motion (in the free draining and weakly bending rod approximation) of a wormlike chain with finite backbone elasticity and gives an outline of the problems of going beyond the weakly bending rod approximation, which was later attempted by Aragón [6, 4, 5]. A closer examination of the weakly bending rod limit was performed by Fujime and Maeda [28], Song *et al.* [88], and Farge and Maggs [22]. Farge and Maggs rederived the stretched exponential law for the tail of the structure factor, which had been obtained in a more general context earlier [26], and applied it to dynamic light scattering experiments in order to determine the persistence length of microfilaments.

5.2 Introduction of the equation of motion

We will now turn to a detailed description of the dynamical model, which we will apply for the calculation of the dynamic structure factor. Since this calculation will be restricted to the case of a long weakly bending rod,

$$\lambda \ll L, \ell_p \quad (26)$$

we discuss the conformational dynamics only in this limit. Hence, we can write the following Langevin equation for the time evolution of the conformation $\mathbf{r}(s, t)$,

$$\frac{\partial \mathbf{r}(s, t)}{\partial t} = \int_0^L ds' \mathbf{H}_\perp [\mathbf{r}(s, t) - \mathbf{r}(s', t)] \left(-\frac{\delta}{\delta \mathbf{r}(s', t)} \mathcal{H}[\mathbf{r}(s', t)] + \mathbf{f}(s', t) \right) . \quad (27)$$

By \mathbf{H}_\perp we denote the *mobility matrix* not to be confused with the Hamiltonian \mathcal{H} of Eq. (1), and $\mathbf{f}(s, t)$ is a thermal random force (per length) with

Gaussian correlations to be specified below. By the mobility matrix we have to account for the hydrodynamic interactions *and* for the rigid constraint. Disregarding the rigid constraint, the mobility matrix would be identical to the *Oseen tensor*

$$\mathbf{H}(\mathbf{r}) = \frac{1}{8\pi\eta r} \left(\mathbf{1} + \frac{\mathbf{r} \otimes \mathbf{r}}{r^2} \right), \quad (28)$$

which is obtained by integrating out (in the Stokes approximation) the hydrodynamics of the pure solvent from the coupled equations of motion of the solvent and the Brownian particles [21]. In presence of the rigid constraint and in the weakly bending rod limit, a heuristic expression for the mobility matrix is [56]

$$\mathbf{H}_\perp(\mathbf{r}) = \frac{1}{8\pi\eta r} \left(\mathbf{1} - \frac{\mathbf{r} \otimes \mathbf{r}}{r^2} \right). \quad (29)$$

In contrast to the Oseen tensor, this definition makes sense only for \mathbf{r} on the polymer contour. The projector onto the polymer axis has the opposite sign as in Eq. (28). While the hydrodynamic interactions favor the longitudinal motion of aligned Brownian particles (by the positive sign of the projector on the molecular axis), we have to suppress this motion completely for a sufficiently long stiff rod (negative sign of the projector). Hence, Eq. (29) amounts to simply “adding” the rigid constraint to the Oseen tensor, i.e., to projecting the Oseen tensor onto the transverse coordinates of the polymer. To recover the free draining approximation we take the parentheses out of the integral in Eq. (27) and perform the integral over \mathbf{H}_\perp in the rod approximation, $|\mathbf{r}(s, t) - \mathbf{r}(s', t)| = |s - s'|$. Thereby we encounter the singular nature of the hydrodynamics of a straight line, i.e., we have to regularize the integral at the lower bound. A possible regularization of the mobility matrix is

$$\tilde{H}_\perp(\mathbf{r}) = \frac{e^{-r/\xi_h} - e^{-r/a}}{8\pi\eta r} \left(\mathbf{1} - \frac{\mathbf{r} \otimes \mathbf{r}}{r^2} \right), \quad (30)$$

where we have introduced along with the microscopic cutoff a (which is of the order of the diameter of the rod) a long wavelength screening length ξ_h . The latter accounts for hydrodynamic screening effects by surrounding molecules. A formal derivation of the hydrodynamic screening term for a semidilute solution of rods has been achieved within an effective medium approach [66]. It is found that ξ_h has the same scaling with concentration c as the mesh size $\xi_m \propto c^{-1/2}$ of the network. We thus obtain an effective

friction coefficient per length

$$\zeta_{\perp}^{\text{screened}} = \frac{4\pi\eta}{\ln(\xi_h/a)} \quad (31)$$

for the transverse excursions of the contour, where we have assumed $L \gg \xi_h \gg a$. A more satisfying procedure to arrive at the free draining approximation is to evaluate the Fourier transform of Eq. (30) with respect to contour length s . We then obtain a mode mobility

$$8\pi\eta H_{\perp}(k) = \frac{1}{2} \ln \left(\frac{a^{-2} + k^2}{\xi_h^{-2} + k^2} \right) \xrightarrow{ka \ll 1} \frac{1}{2} \ln \left(\frac{a^{-2}}{\xi_h^{-2} + k^2} \right) \quad (32)$$

for transverse undulations.⁶ The latter is logarithmically mode dependent, weak enough that we may approximate it by a constant effective mobility ζ_{\perp}^{-1} . In Section 6.2 we will show how this effective mobility coefficient can be fixed to a reasonable value. We summarize the preceding discussion by concluding that the weakly bending rod approximation allows one to respect the rigid constraint and the hydrodynamic interactions in a fairly good approximation without going beyond the simple linear Langevin equation for the transverse undulations $\mathbf{r}_{\perp}(s, t)$ already proposed by Soda [86],

$$\zeta_{\perp} \frac{\partial \mathbf{r}_{\perp}(s, t)}{\partial t} = -\kappa \frac{\partial^4 \mathbf{r}_{\perp}(s, t)}{\partial s^4} + \mathbf{f}^{\perp}(s, t). \quad (33)$$

To linear order there is no fluctuation of the longitudinal coordinate $\mathbf{r}_{\parallel} = s$ along the axis of the weakly bending rod. The transverse stochastic forces are assumed to have Gaussian correlations with

$$\langle f_i^{\perp}(s, t) f_j^{\perp}(s', t') \rangle = 2k_B T \zeta_{\perp} \delta^{ij} \delta(s - s') \delta(t - t'). \quad (34)$$

In the remainder of this subsection we give a brief qualitative discussion of the major consequences of Eq. (33) for the dynamics of a wormlike chain and a simplified outline of the more formal considerations in the following sections.

From Eq. (33) we immediately read off the characteristic relaxation time of the transverse undulations of wavelength l

$$\tau_l = \frac{\zeta_{\perp}}{\kappa} l^4. \quad (35)$$

⁶According to the definitions in Subsection 5.3 the mode friction is by a factor of two larger than the real space friction coefficient per length. Please do not confuse the mode number k with the scattering vector q .

From this we can already deduce the characteristic decay rate of the structure factor of a stiff semiflexible polymer by a scaling argument [22]. We expect a mode of wavelength of about l to contribute most to the decay at time $t \simeq \tau_l$. By use of Eq. (35) we can solve this equation for l . Recalling the result $r_{\perp}^2 \propto l^3/\ell_p$ of Eq. (7) for the self-affine scaling of the transverse excursions of a stiff polymer we find for the mean-square displacement

$$\delta r_{\perp}^2(t) := \langle [r_{\perp}(t) - r_{\perp}(0)]^2 \rangle \propto \left(\frac{k_B T}{\zeta_{\perp} \ell_p^{1/3}} t \right)^{3/4}. \quad (36)$$

The decay of the structure factor is caused by these transverse undulations. Assuming that it is directly determined by the mean-square displacement via $S(q, t) \propto \exp[-q^2 \delta r_{\perp}^2(t)/4]$ (which is only true for long times) we anticipate the stretched exponential tail derived below. It is probably due to this suggestive scaling argument that the latter has been derived by so many authors [26, 22, 33, 37, 56, 34]. It has been confirmed experimentally with very high accuracy for semidilute actin solutions [33]. Recently, the sub-diffusive growth of the transverse mean-square displacement $\delta r_{\perp}^2(t)$ has also been demonstrated in real space for microtubuli [15]. Similar results have been reported for the center of mass motion of a bead with diameter d embedded in an actin solution with a mesh size smaller than the bead diameter [3]. It is argued that even if the bead is interacting with several filaments this will only change prefactors but not the exponents of the anomalous diffusion law.

Up to now we have neglected interactions between filaments in our considerations. Though complicated in reality, these interactions are commonly represented by a simple cylindrically shaped mean field potential [71] added to Eq. (1). Such a model is suggested by direct fluorescence microscopy studies with actin [49] that visualize the tube-like confinement of single fluorescent actin filaments in a semidilute solution of unlabeled filaments. (However, it would be too naive to interpret the volume traced over time by the labeled polymer as the quasi-static confining ‘tube’ of a single fluctuating test polymer. One also has to consider the dynamics of the surrounding polymer network). We can again apply simple scaling arguments to anticipate the effect of a harmonic confinement potential on the transverse mean-square displacement Eq. (36). In the presence of a linear confinement force $-\sigma \mathbf{r}_{\perp}$ on the right hand side of Eq. (33) the characteristic relaxation time of Eq. (35) becomes $\tau_l^e = \zeta_{\perp}/(\kappa/l^4 + \sigma)$ and the *confined* mean-square displacement

$\delta r_{\perp}^2(\sigma, t)$ reads

$$\delta r_{\perp}^2(\sigma, t) = \delta r_{\perp}^2(0, t)F(\sigma t/\zeta_{\perp}) , \quad (37)$$

where $\delta r_{\perp}^2(0, t) \equiv \delta r_{\perp}^2(t)$ is given by Eq. (36). We have introduced a scaling function $F(x)$ which reduces to one for $x \rightarrow 0$ and enforces the confinement (i.e. time independence of $\delta r_{\perp}^2(\sigma, t)$ for long times) via $F(x \rightarrow \infty) = x^{-3/4}$. The characteristic crossover time $\tau_0^e := \zeta_{\perp}/\sigma$ is the typical relaxation time of the shortest mode that is substantially hindered by the confining tube. Assuming a static tube, we have still neglected the motion of the surroundings. In the following sections we will recover the above scaling predictions from a more quantitative analysis of Eq. (33) and also consider dynamic contributions from the surrounding polymer network. We will not consider single chain reptation, which is the conventional mechanism for interpreting the tail of the structure factor in the case of flexible polymers [18, 75, 42]. The contributions of reptation to the de-correlation of the scattering signal are less (if at all) relevant in the limit of interest ($\lambda \ll L, \ell_p$).

5.3 Linear mode analysis

The linear Langevin Equation Eq. (33) can be solved by linear mode analysis for different boundary conditions. Here, we do not give a full account of all ten possible boundary problems, but refer the interested reader to Ref. [95]. As we are mainly interested in the internal dynamics of polymers we focus our attention onto polymers that are much longer than the scattering wavelength $\lambda = 2\pi/q$, which implies that the precise form of the boundary conditions is irrelevant for our final results (and only in this limit the final results have a simple form). We take advantage of this situation to consider particularly simple boundary conditions, namely *hinged ends*. This corresponds to a polymer with its ends held by optical traps or freely rotating crosslinks. Other boundary conditions can be implemented with some more writing by the same procedure.

Now, we look for the solution $r_{\perp}(s, t)$ (which stands for one component of the local transverse deviation \mathbf{r}_{\perp} of the contour from its average axis) of the linear equation

$$\zeta_{\perp} \frac{\partial}{\partial t} r_{\perp}(s, t) = -\kappa \frac{\partial^4}{\partial s^4} r_{\perp}(s, t) \quad (38)$$

subject to the condition of hinged ends

$$r_{\perp}(s, t)|_{\mathcal{B}} = 0 \quad \text{and} \quad \frac{\partial^2}{\partial s^2} r_{\perp}(s, t)|_{\mathcal{B}} = 0. \quad (39)$$

The notation $|_{\mathcal{B}}$ refers to the boundaries at $s = 0$ and $s = L$. We introduce formally the complete set of eigenfunctions $\psi_n(s)$, which exists because of the self-adjoint property of the differential operator $\partial^4/\partial s^4$. We multiply Eq. (38) by the n^{th} eigenfunction $\psi_n(s)$ and integrate over s from 0 to L ,

$$\frac{\partial}{\partial t} \int ds \psi_n r_{\perp} = -\frac{\kappa}{\zeta_{\perp}} \int ds \psi_n \frac{\partial^4}{\partial s^4} r_{\perp} = -\frac{\kappa}{\zeta_{\perp}} \int ds r_{\perp} \frac{\partial^4}{\partial s^4} \psi_n + \mathcal{B}. \quad (40)$$

By \mathcal{B} we abbreviate the eight boundary terms generated by partial integration. Four of these boundary terms vanish as a direct consequence of Eq. (39), the others because the eigenfunctions ψ_n have to satisfy the same boundary conditions. Together with Eq. (40) the latter implies that the eigenfunctions are ordinary Fourier modes

$$\psi_n(s) = \frac{1}{L} \sin \frac{n\pi s}{L} \quad (41)$$

for natural numbers n . In general the eigenfunctions are linear combinations of sin, cos, sinh, cosh, and the eigenvalues are given as the infinite set of solutions of a transcendental equation. The spectral decomposition of $r_{\perp}(s, t)$ into the Fourier modes $\psi_n(s)$ defines the mode amplitudes

$$\tilde{r}_{\perp}(n, t) := \int ds r_{\perp}(s, t) \psi_n(s). \quad (42)$$

Using the inversion of Eq. (42),

$$r_{\perp}(s, t) = 2L \sum_n \tilde{r}_{\perp}(n, t) \psi_n(s) \quad (43)$$

in the equation of motion, Eq. (38), or directly from Eq. (40) we obtain

$$\tilde{r}_{\perp}(n, t) = \tilde{r}_{\perp}(n, 0) \exp(-t/\tau_n). \quad (44)$$

We have introduced the characteristic decay time of the n^{th} mode

$$\tau_n := \frac{\tau_L}{(n\pi)^4} \equiv \frac{\zeta_{\perp}}{\kappa} \left(\frac{L}{n\pi} \right)^4, \quad (45)$$

with $\tau_L = \zeta_\perp L^4 / \kappa$ as in Eq. (35). The cross-correlation of the mode amplitudes is

$$\langle \tilde{r}_\perp(n, t) \tilde{r}_\perp(m, 0) \rangle = \delta_{nm} \langle \tilde{r}_\perp^2(n, 0) \rangle \exp(-t/\tau_n). \quad (46)$$

The static mean-square amplitudes are determined from the equipartition theorem

$$\langle \tilde{\mathbf{r}}_\perp^2(n, 0) \rangle = \frac{k_B T L^3}{\kappa (n\pi)^4}, \quad (47)$$

where the boldface notation emphasizes that \mathbf{r}_\perp comprises two independent degrees of freedom. Now we can proceed calculating other correlation functions such as the reduced cross-correlation of the transverse segment undulations

$$r_{ss'}^{\perp 2}(t) := \langle [\mathbf{r}_\perp(s, t) - \mathbf{r}_\perp(s', 0)]^2 \rangle, \quad (48)$$

which we rewrite as

$$\begin{aligned} r_{ss'}^{\perp 2}(t) &= r_{ss'}^{\perp 2} + \delta r_{ss'}^{\perp 2}(t) \\ &= \langle [\mathbf{r}_\perp(s, 0) - \mathbf{r}_\perp(s', 0)]^2 \rangle \\ &\quad + 2 \langle \mathbf{r}_\perp(s, 0) \mathbf{r}_\perp(s', 0) - \mathbf{r}_\perp(s, t) \mathbf{r}_\perp(s', 0) \rangle. \end{aligned} \quad (49)$$

The first term is purely static, cf. Eq. (7), while the second term vanishes for $t \rightarrow 0$. We introduce the mode decomposition of $\mathbf{r}_\perp(s, t)$ from Eq. (43) in the last expression of Eq. (49) to obtain

$$\delta r_{ss'}^{\perp 2}(t) = 4 \sum_n \langle \tilde{\mathbf{r}}_\perp^2(n, 0) \rangle (1 - e^{-t/\tau_n}) \cos[n\pi(s - s')/L], \quad (50)$$

where we have dropped a rapidly oscillating term $\propto \cos[n\pi(s + s')/L]$. For times $t \ll \tau_L$ we can perform the continuum limit replacing the sum by an integral, and applying the equipartition theorem, Eq. (47), we finally obtain

$$\delta r_{ss'}^{\perp 2}(t) = \frac{4L^3}{\ell_p} \int_0^\infty dn \frac{(1 - e^{-t/\tau_n})}{(n\pi)^4} \cos\left(\frac{n\pi}{L}(s - s')\right). \quad (51)$$

The diagonal elements $\delta r_\perp^2(t) := \delta r_{ss}^{\perp 2}(t)$ represent the *mean-square segment displacement*

$$\delta r_\perp^2(t) = \frac{4\Gamma(1/4)}{3\pi} \left(\frac{k_B T}{\zeta_\perp \ell_p^{1/3}} t \right)^{3/4}, \quad (52)$$

where we have used the identity

$$\int_0^\infty dz \frac{1 - e^{-z^4}}{z^4} = \frac{\Gamma(1/4)}{3}. \quad (53)$$

We have thus recovered the scaling prediction from Eq. (36) up to a numerical prefactor of $4\Gamma(1/4)/3\pi \approx 1.539$. As we noted above, $\delta r_\perp^2(t)$ can directly be measured for large biomolecules such as microtubuli [15]. The fact that $\delta r_\perp^2(t)$ is independent of s is a consequence of assuming an infinitely long polymer and discarding the term containing $s + s'$ in Eq. (51).

5.4 Entanglement effects

Above, we have discussed the dynamics of a single wormlike chain. In cases of practical interest, stiff polymers are rarely encountered in isolation but rather in semidilute solutions. Due to the low volume fraction of thin long rods, a dilute solution, in which these rods do not overlap, does not give a sufficient scattering intensity. One is thus forced to study semidilute solutions, which contain a dense mesh-work of polymers similar to that in Fig. 1. Even in the presence of mutual steric and hydrodynamic interactions the single polymer picture still applies when the scattering wavelength λ is much smaller than the characteristic *mesh size* ξ_m of the network. The decay of the structure factor is then mostly due to modes that are not hindered by the surroundings. However, if the condition $\lambda \ll \xi_m$ does not hold, the structure factor will show deviations from the simple form derived for a single polymer in Sections 6.2-6.3. The strongest deviations occur at small scattering angles and long times, where the interactions of the polymer with its surroundings are most pronounced.

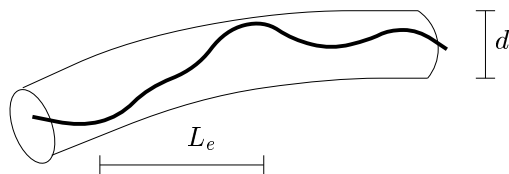


Figure 6: The tube-like confinement of a single test polymer by the surrounding network is most simply described by a cylindrically shaped confining potential. However, the dynamics of the surroundings can not be neglected.

A simple method to account for hydrodynamic screening effects has already been discussed in Subsection 5.2, i.e., the mode number dependence of the friction coefficient saturates at a screening length ξ_h of about the mesh size of the network [66, 56]. The steric constraints are very complicated in reality, but are often represented by an effective tube-like cage [71] depicted in Fig. 6. The cage is readily implemented in the theoretical analysis by adding to the right hand side of Eq. (33) a harmonic restoring force $-\sigma \mathbf{r}_\perp(s, t)$, which keeps the transverse undulations from growing infinitely. Modes of wavelength longer than the *entanglement length* or *deflection length* [71]

$$L_e := (\kappa/\sigma)^{1/4} \quad (54)$$

are strongly damped, because they interfere with the long wavelength modes of the surrounding polymers represented by the tube potential. For the number of ‘entanglement segments’ L/L_e of a polymer we will also write n_e . The *confined* mean-square displacement $r_\perp^2(\sigma, t)$, which dominates the tail of the structure factor (cf. Section 6.3), is given by

$$\begin{aligned} \delta r_\perp^2(\sigma, t) &= \frac{4L^3}{\ell_p} \int_0^\infty dn \frac{1 - e^{-t/\tau_n^e}}{(n\pi)^4 + n_e^4} \\ &= \delta r_\perp^2(0, t) \frac{3\Gamma(3/4, 0, t/\tau_0^e)}{4(t/\tau_0^e)^{3/4}} \\ &= \frac{\sqrt{2}L_e^3}{\ell_p} \left(1 - \frac{\Gamma(3/4, t/\tau_0^e)}{\Gamma(3/4)} \right). \end{aligned} \quad (55)$$

As a generalization of the decay time τ_n of Eq. (45) we have introduced the new characteristic relaxation time

$$\tau_n^e := \frac{\tau_L}{(n\pi)^4 + n_e^4}, \quad (56)$$

for the Brownian motion in the cage potential. The relaxation time

$$\tau_0^e = \frac{\zeta_\perp}{\sigma} = \frac{\zeta_\perp L_e^4}{\kappa} \quad (57)$$

of a mode of wavelength $\approx 2L_e$ defines the time scale where the constraints become active. The (generalized) incomplete Γ -functions are defined as

$$\Gamma(a, 0, z) := \int_0^z dt t^{a-1} e^{-t}, \quad \Gamma(a, z) := \int_z^\infty dt t^{a-1} e^{-t}. \quad (58)$$

The expressions given in the second/third line of Eq. (55) are useful for short/long times t with respect to τ_0^e . The deviations from the free mean-square displacement $\delta r_{\perp}^2(0, t) \equiv \delta r_{\perp}^2(t)$ of Eq. (51) grow as

$$\delta r_{\perp}^2(\sigma, t)/\delta r_{\perp}^2(0, t) = 1 - \frac{3t}{7\tau_0^e} + \mathcal{O}(t^2) \quad (59)$$

for $t \ll \tau_0^e$. For long times $t \gg \tau_0^e$ the last term in the third line of Eq. (55) vanishes and the mean-square displacement saturates at a plateau value, $\delta r_{\perp}^2(\sigma, t \rightarrow \infty) = \sqrt{2}L_e^3/\ell_p$, see Fig. 7. Additionally, we should consider the possible constraints at the ends of a certain part of the chain. These may occur in a solution due to inhomogeneities of the tube (which, in reality, is not a homogeneous cylinder as assumed by our simple ansatz) or from chemical crosslinks in a gel. As long as the chemical distance between two adjacent constraints is still large compared to the scattering wavelength, they can be taken into account perturbatively by introducing a nonzero lower bound of the integral in Eq. (55). The leading order correction to the mean-square displacement in Eq. (51) is linear in t [56], and therefore not identical to the leading order correction from the tube constraint, which is proportional to $\delta r_{\perp}^2(0, t) \cdot t/\tau_0^e \propto t^{7/4}$ according to Eq. (59). For a more rigorous analysis, we should go back to the linear mode analysis of Section 5.3 and apply the appropriate boundary conditions for a particular sort of crosslinks, also taking care of the elastic forces (tension along the filament) generated by the surrounding network.

It seems, however, more important to realize that the surroundings will not provide a *static* cage, but will itself be subject to the collective dynamics of the solution⁷. The latter are most simply described by a diffusion equation for the overdamped phonons of a homogeneous effective medium. The elastic properties of the latter are characterized by an osmotic compressibility K and a shear modulus μ . The equation of motion of the displacement of a point in the medium subject to the random force density $\mathbf{f}(\mathbf{x}, t)$ is (for low volume fraction of polymers) [90, 29]

$$\zeta \frac{\partial}{\partial t} \mathbf{r} = \left(K + \frac{\mu}{3} \right) \nabla(\nabla \mathbf{r}) + \mu \nabla^2 \mathbf{r} + \mathbf{f}. \quad (60)$$

We do not enter the discussion of the relation of the elastic constants and the friction coefficient ζ of the effective medium to single polymer properties

⁷As noted before, working in the limit $\lambda \ll L, \ell_p$, we are neglecting contributions to the mean-square displacement from reptational motion of the chain along the tube.

but consider them as independent phenomenological constants here. The displacement vector \mathbf{r} can be decomposed into a rotation free and a divergence free component, \mathbf{r}_l and \mathbf{r}_t , respectively.⁸ Both obey diffusion equations with the respective diffusion coefficients

$$D_l := (K + 4\mu/3)/\zeta \quad (\text{longitudinal}) \quad (61)$$

$$D_t := \mu/\zeta \quad (\text{transverse}) . \quad (62)$$

The contribution of the collective modes to the local mean-square displacement of a single polymer is calculated from these diffusion equations as

$$\delta r_{\perp}^2(t) = \frac{4}{3} \int_0^{k_c} \frac{k^2 dk}{2\pi^2} \left[\langle \mathbf{r}_k^t \mathbf{r}_{-k}^t \rangle \left(1 - e^{-k^2 D_t t} \right) + 2 \langle r_k^l r_{-k}^l \rangle \left(1 - e^{-k^2 D_l t} \right) \right] . \quad (63)$$

(A factor of 2/3 is due to the projection of the isotropic mean-square displacement of the surroundings onto the plane perpendicular to the polymer axis.) After applying the equipartition theorem and evaluating the integrals we obtain for the mean-square displacement

$$\delta r_{\perp}^2(t) = \frac{4}{3} \langle \mathbf{r}_t^2 \rangle \left(1 - \sqrt{\pi} \frac{\text{erf}(\sqrt{\omega_e^{t,t}})}{2\sqrt{\omega_e^{t,t}}} \right) + \frac{4}{3} \langle r_l^2 \rangle \left(1 - \sqrt{\pi} \frac{\text{erf}(\sqrt{\omega_e^{l,t}})}{2\sqrt{\omega_e^{l,t}}} \right) . \quad (64)$$

Here $\omega_e^{t,l} := k_c^2 D_{t,l}$ are the characteristic relaxation rates for transverse and longitudinal collective modes, respectively, and k_c is the high wave number cutoff for the effective medium description. This cutoff length also determines the magnitude of the static transverse and longitudinal fluctuations,

$$\langle r_l^2 \rangle = \frac{k_B T}{2\pi(K + 4\mu/3)} \frac{k_c}{\pi} , \quad \langle \mathbf{r}_t^2 \rangle = \frac{k_B T}{\pi\mu} \frac{k_c}{\pi} . \quad (65)$$

For long times $t \gg 1/\omega_e^{l,t}$ the error functions saturate and the relaxation of the mean-square displacement becomes algebraically slow.

It is not yet clear how the crossover between the single polymer dynamics and the collective modes occurs in detail. Possibly, the simple tube model discussed above is too naive. It is conceivable that the crossover to the three dimensional (homogeneous) effective medium is slow, i.e., that there

⁸The reader should not confuse the longitudinal and transverse components \mathbf{r}_l and \mathbf{r}_t of the displacement vector of the effective medium with longitudinal and transverse coordinates r_{\parallel} and \mathbf{r}_{\perp} of the contour of a single polymer.

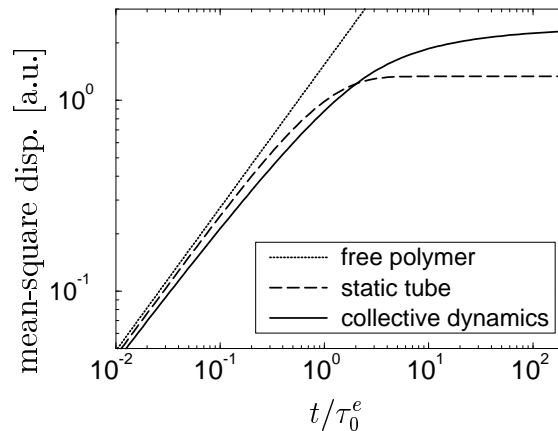


Figure 7: Mean-square displacement of a wormlike chain. The curves correspond to the free chain Eq. (52), the chain in a static tube-like harmonic potential Eq. (55) and the chain in a tube with collective background dynamics according to Eq. (66), respectively.

are intermediate steps where the inhomogeneous effective medium has to be described in terms of fractal dimensions. To compare the theory to experimental data, we make the simplifying assumption $\omega_e^t = \omega_e^l = \omega_* = 1/\tau_0^e$ to reduce the number of free parameters. Here ω_* is to be regarded as an effective phenomenological crossover rate not strictly identical to $1/\tau_0^e$ as defined in Eq. (57). The mean-square displacement $\delta r_{\perp}^2(\omega_* t)$ for the coupled model of Eq. (60) and Eq. (33) thus becomes [57]

$$\begin{aligned} \delta r_{\perp}^2(\omega_* t) = & \frac{4}{3} \langle \mathbf{r}^2 \rangle \left[1 - \sqrt{\pi} \frac{\text{erf}(\sqrt{\omega_* t})}{2\sqrt{\omega_* t}} \right] \\ & + \frac{4}{3\pi} \left(\frac{k_B T \omega_*^{-1}}{\zeta_{\perp} \ell_p^{1/3}} \right)^{3/4} \left[1 - (\omega_* t)^{3/4} \frac{3}{4} \Gamma[-3/4, \omega_* t] \right]. \end{aligned} \quad (66)$$

The prefactors in front of the brackets [...] correspond to two times the (projected) mean-square fluctuations of the polymer in its tube and of the effective medium, respectively. Eq. (66) is also plotted in Fig. 7. The saturation of the mean-square displacement is much slower than in the static tube model of Eq. (55) if the collective modes of the medium are taken into account. As we mentioned above, an even slower approach to the plateau at long times can be expected in case of a gradual dimensional crossover,

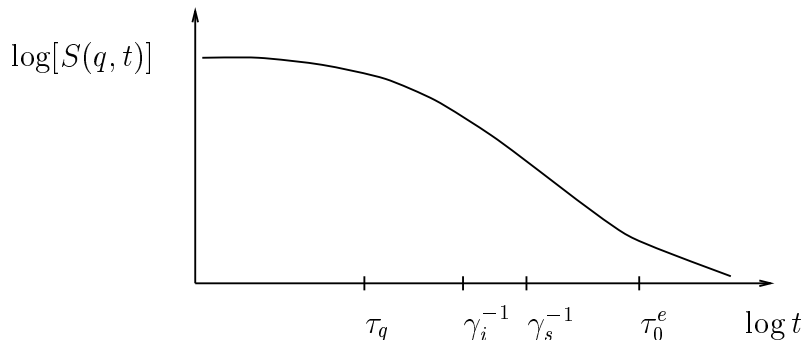


Figure 8: A schematic sketch of the dynamic structure factor of a semiflexible polymer with $\ell_p \gg \lambda$. The crossover time τ_q separates the simple exponential initial decay with characteristic decay rate γ_i from the stretched exponential tail with characteristic decay rate γ_s . For $\ell_p \rightarrow \lambda$ the times τ_q and γ_i^{-1} shift towards γ_s^{-1} . In semidilute solutions the decay of the structure factor is slowed down at long times $t \approx \tau_0^e$ by steric interactions with the surroundings.

which presumably is not properly described by the present approximation of a single crossover frequency ω_* .

6 Dynamic structure factor

Dynamic scattering techniques have become a powerful tool for measuring dynamics of polymeric and colloidal systems over many decades in time [9, 82, 13, 42]. The range of problems accessible to scattering methods has been extended by the increased capacity of the more conventional neutron and light scattering methods and also by development of new techniques such as diffusing-wave spectroscopy [94]. Scattering measurements complement the information provided by other techniques such as birefringence measurements, chromatography, rheology etc., and recently developed microscopic real space methods such as micro-rheology and video microscopy of fluorescence labeled polymers. In contrast to the more direct microscopic methods, dynamic scattering experiments average over a sample of molecules of all possible orientations and conformations with all kinds of dynamic modes excited by thermal noise. As a consequence, the calculation of the dynamic structure factor involves such an averaging procedure, which is a complicated task in general. However, this task is greatly facilitated in the limit of (randomly oriented) long weakly bending rods ($\lambda \ll \ell_p, L$), which we consider here.

6.1 Definitions

Before going into the calculation we introduce the characteristic time scales

$$\begin{aligned}
 \tau_q &:= \frac{\zeta_{\perp}}{\kappa q^4}, \\
 \gamma_i &:= (q\ell_p \tau_q)^{-1} \equiv \frac{k_B T}{\zeta_{\perp}} q^3 \\
 \gamma_s &:= (q\ell_p)^{-4/3} \tau_q^{-1} \equiv \frac{k_B T q^{8/3}}{\zeta_{\perp} \ell_p^{1/3}}.
 \end{aligned} \tag{67}$$

The time τ_q can be interpreted as the characteristic relaxation time of a mode of wavelength $2\pi/q$. The two relaxation rates γ_i and γ_s will turn out to be (up to numerical prefactors) the *initial decay rate* and the *decay rate of the stretched exponential tail*, respectively. The main result of the present section will be that the dynamic structure factor has a simple exponential initial decay $\exp[-c_1 \gamma_i t]$ followed by a stretched exponential tail $\exp[-c_2 (\gamma_s t)^{3/4}]$ where c_1 and c_2 are numerical constants (see Fig. 8). Which of these decay laws actually dominates the structure factor depends on the relative magnitude of the initial decay rate γ_i and the *crossover time* τ_q . For small $\gamma_i \tau_q = (q\ell_p)^{-1}$ (the limit, where the derived results become exact) the stretched exponential decay is dominant. On the other hand, for $q\ell_p \rightarrow 1$ the two decay rates γ_i and γ_s approach the same value τ_q^{-1} and the stretched exponential tail is shifted to long times, where the scattering function is already small.

The coherent dynamic structure factor (the intermediate scattering function) of a *single* polymer is defined as

$$S(\mathbf{q}, t) = \frac{1}{N} \sum_{n m} \langle e^{i\mathbf{q}[\mathbf{r}_n(t) - \mathbf{r}_m(0)]} \rangle, \tag{68}$$

where the sum is over all N ‘monomers’ (contour elements represented as point scatterers) along the polymer. We take advantage of the fact that we are concerned with a long weakly bending rod to split the coordinates \mathbf{r} and the scattering vector \mathbf{q} into components r^{\parallel} , q^{\parallel} and \mathbf{r}^{\perp} , \mathbf{q}^{\perp} parallel and transverse to the contour, respectively. Accordingly, we split the statistical average into a thermal average $\langle \dots \rangle_T$ over the transverse undulations driven by the random forces and an orientational average $\langle \dots \rangle_O$ over the quasi-static

orientation of the rod axis. We thus rewrite the right hand side of Eq. (68) as

$$\frac{1}{N} \sum_{nm} \left\langle \left\langle e^{i\mathbf{q}^\perp [\mathbf{r}_n^\perp(t) - \mathbf{r}_m^\perp(0)]} \right\rangle_T e^{iq^\parallel [r_n^\parallel - r_m^\parallel]} \right\rangle_O . \quad (69)$$

Note that the longitudinal coordinates are independent of time for a weakly bending rod and hence can be taken out of the thermal average. Because the random forces are assumed to have Gaussian correlations we may rewrite this in the form

$$\frac{1}{N} \sum_{nm} \left\langle e^{-q^\perp r_{nm}^{\perp 2}(t)/4} e^{iq^\parallel a(n-m)} \right\rangle_O \quad (70)$$

with $r_n^\parallel = an$ and the short-hand notation $r_{nm}^{\perp 2}(t)$ for the reduced cross-correlation of the transverse segment undulations from Eq. (48). (One may think of a as the monomer size.) Next we substitute the explicit form of the orientational average by introducing the angle θ to the rod axis. With $q^\parallel = q \cos \theta$, $q^\perp = q \sin \theta$, $\langle \dots \rangle_O = 1/2 \int_0^\pi d\theta \sin \theta (\dots)$ and $x := \cos \theta$ we thus obtain

$$S(q, t) = \frac{1}{2N} \sum_{nm} \int_{-1}^1 dx e^{-(1-x^2)q^2 r_{nm}^{\perp 2}(t)/4} e^{iqxa(n-m)} . \quad (71)$$

The transverse undulations $r_{nm}^{\perp 2}(t)$ can be further decomposed into a static and dynamic contributions as in Eq. (49)

$$\begin{aligned} r_{nm}^{\perp 2}(t) &= r_{nm}^{\perp 2} + \delta r_{nm}^{\perp 2}(t) \\ &= \langle [\mathbf{r}_\perp(n, 0) - \mathbf{r}_\perp(m, 0)]^2 \rangle_T \\ &\quad + 2 \langle \mathbf{r}_\perp(n, 0) \mathbf{r}_\perp(m, 0) - \mathbf{r}_\perp(n, t) \mathbf{r}_\perp(m, 0) \rangle_T . \end{aligned} \quad (72)$$

6.2 Initial decay ($t \ll \tau_q$)

We expand the time dependent part of $S(q, t)$ into its Taylor series, the higher order terms of which we abbreviate by (\dots) for convenience of presentation,

$$\frac{1}{2N} \sum_{nm} \int_{-1}^1 dx [1 - (1-x^2)q^2 \delta r_{nm}^{\perp 2}(t)/4 + \dots] e^{iqxa(n-m) + (1-x^2)q^2 r_{nm}^{\perp 2}} . \quad (73)$$

The zeroth order is of course nothing but the static structure factor $S(q) \equiv S(q, 0)$. Disregarding the term $r_{nm}^{\perp 2}$ in the exponent we recover the expression for a rigid rod, Eq. (18) of Section 2. To analyze further the dynamic part

of the structure factor, $S(q, t) - S(q)$, we need the explicit expression for $\delta r_{nm}^{\perp 2}(t)$ which was calculated in Section 5.3. With the notation introduced in Eq. (67) we rewrite Eq. (51) of Section 5.3 in the form

$$q^2 \delta r_{nm}^{\perp 2}(t)/4 = \frac{(\gamma_s t)^{3/4}}{\pi} \int_0^\infty \frac{dz}{z^4} (1 - e^{-z^4}) \cos \left(\frac{zqa(n-m)}{(t/\tau_q)^{1/4}} \right). \quad (74)$$

To first order we thus have

$$S(q, t) - S(q) = -\frac{(\gamma_s t)^{3/4}}{2N\pi} \sum_{nm} \int_{-1}^1 dx (1 - x^2) \int_0^\infty \frac{dz}{z^4} (1 - e^{-z^4}) \\ \times \exp [iqa(n-m)(x + z/(t/\tau_q)^{1/4}) + (1 - x^2)q^2 r_{nm}^{\perp 2}]. \quad (75)$$

For short times $t \ll \tau_q$, the term proportional to $z/(t/\tau_q)^{1/4}$ dominates the exponential in the second line of the last equation. Neglecting the static terms in the exponential, it simplifies to

$$S(q, t \rightarrow 0) - S(q) = -\frac{2(\gamma_s t)^{3/4}}{3N\pi} \int_0^\infty \frac{dz}{z^4} (1 - e^{-z^4}) \frac{\sin^2[qLz/2(t/\tau_q)^{1/4}]}{[qaz/2(t/\tau_q)^{1/4}]^2}. \quad (76)$$

The last term is strongly peaked for short times, rendering the structure factor to first order as

$$S(q, t \rightarrow 0) - S(q) = -2\gamma_i t/3qa, \quad (77)$$

with the characteristic decay rate γ_i introduced in Eq. (67). We finally substitute for the static structure factor its asymptotic form for large qL , $q\ell_p$ from Eq. (19), $S(q) \sim \pi/qa$, to obtain for the initial decay of the dynamic structure factor

$$\frac{S(q, t \rightarrow 0)}{S(q)} = 1 - \frac{2k_B T}{3\pi\zeta_\perp} q^3 t \quad (t \ll \tau_q, \lambda \ll \ell_p, L). \quad (78)$$

In brackets we have indicated the range of validity for this result. We conclude that the initial decay of the dynamic structure factor of a long weakly bending rod is of the form

$$\frac{S(q, t)}{S(q)} = \exp \left(-\frac{2}{3\pi} \gamma_i t \right) \quad (t \ll \tau_q). \quad (79)$$

The time region of validity of this result is smaller than the inverse initial decay rate γ_i^{-1} , and hence it gives only an asymptotic short time limit in the case of large $q\ell_p$. However, we expect that Eq. (79) remains at least qualitatively valid for more flexible polymers with $q\ell_p \approx 1$. In that case, Eq. (79) predicts a mainly simple exponential decay of $S(q, t)$.

Comparing Eq. (78) with a calculation of the initial decay rate from a Smoluchowski equation equivalent to Eq. (27) we can estimate the effective friction coefficient ζ_\perp introduced in Eq. (33). Within the approach from the Smoluchowski equation no approximation of the hydrodynamic friction is needed and the full Oseen tensor can be used. The price one has to pay is that the rigid constraint of constant tangent length is not easily implemented. In Ref. [56] we proposed a heuristic argument to cure this deficiency. We postpone the technical details to Appendix A and quote the result from Eq. (101),

$$\gamma^{(0)} := - \left. \frac{d \log S(\mathbf{q}, t)}{dt} \right|_0 = \frac{k_B T \ln(e^{5/6}/qa)}{6\pi^2 \eta} q^3. \quad (80)$$

By comparison with Eq. (78), this suggests

$$\zeta_\perp = \frac{4\pi\eta}{\ln(e^{5/6}/qa)} \quad (81)$$

for the effective transverse friction per length of a semiflexible polymer in dilute solution. The dependence of ζ_\perp on the lateral diameter, which enters the calculation as an ultra-violet cutoff, should not come as a surprise, cf. Eq. (32). It is a direct consequence of the tendency of the reciprocal distance law of the hydrodynamic interaction to give large weight to short distances. Together with the (singular) rod-like structure of the polymer this leads within the Smoluchowski equation approach to an integral expression for the first cumulant $\gamma^{(0)}$ that diverges logarithmically at the upper bound. This implies that the main contributions to the integral come from large wave vectors and thus justifies *a posteriori* the weakly bending rod approximation, since even rather flexible polymers become rod-like on short length scales. It also sheds some light on the question, how much one should trust the classical result for the first cumulant of flexible chains (see e.g. the book by Doi and Edwards [21]) when dealing with *real* polymers. For flexible polymers the decay rate is also expressed by an integral over modes, which is, however, convergent at the upper bound. Of course, the convergence of the expression is a consequence of ignoring the local rod-like structure of

real polymers and representing them as fractal Gaussian chains down to the smallest length scales. This is only justified in the limit $L/\ell_p \rightarrow \infty$, which is hard to attain experimentally. The incapability of the result to explain quantitatively the experimental data has been known for years [80, 20]. It is a consequence of non-negligible persistence lengths of the molecules, in other words, “it is no use interpreting data in terms of Gaussian chains when on the scale of observation the chains are no longer behaving as Gaussians” [42]. In more recent neutron scattering studies comparison is usually made with the theory by Akcasu *et al.* [2] for the initial decay rate. However, an attempt to interpret neutron scattering from common ‘flexible’ polymers with $\ell_p \approx q^{-1}$ in terms of Eq. (80) could be worthwhile. Some successful applications of Eq. (80) to dynamic light scattering data will be mentioned below.

Historically, experimental results have often been summarized in terms of the dynamic exponent z characterizing the dispersion relation $\gamma^{(0)}(q) \propto q^z$. To relate the above results to these experiments we can extract this dynamic exponent from the derived expression for the initial decay rate Eq. (80). Due to the logarithmic wave vector dependence of $\gamma^{(0)}$ the effective exponent is weakly q -dependent

$$z(k) = 3 \frac{6 \ln qa - 3}{6 \ln qa - 5}. \quad (82)$$

This function together with a modified expression for a semidilute solution is plotted in Fig. 9 taken from [56]. The limiting value $z = 3$ of the flexible polymer models is recovered in the limit $qa \rightarrow 0$. The slow logarithmic convergence is in accord with the low z values reported in the experimental literature (see de Gennes’ book [17] for a brief summary).

The results of this subsection and Appendix A are not only of academic interest but can be of practical use. The fact that the diameter a of the molecule enters Eq. (80) can be used to determine this model parameter from the dynamic structure factor for polymers with $q\ell_p \approx 1$ but $qa \ll 1$. The method has in fact been shown to give rather accurate results for fibrin and intermediate filaments [7, 48, 65, 43]. Actin filaments are probably too stiff to obtain an accurate value for a in the same way, but the agreement of Eq. (80) with experimental data is still very good [33]. For some more details see Section 6.6.

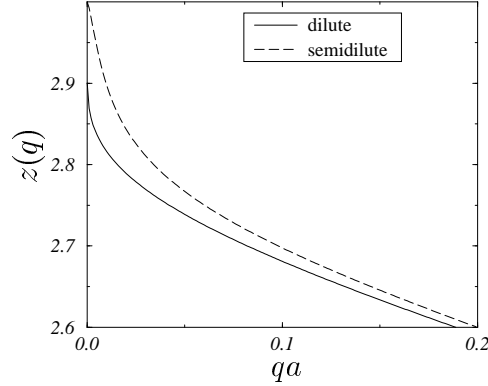


Figure 9: The effective dynamic exponent z that characterizes the dispersion relation $\gamma^{(0)}(q) \propto q^z$. Solid line: Eq. (82), broken line: a representative curve for a semidilute solution with screened hydrodynamic interactions as introduced in Appendix A.

6.3 Stretched exponential decay ($t \gg \tau_q$)

For times longer than the crossover time τ_q introduced in Eq. (67) we will now derive the stretched exponential tail of the scattering function anticipated by the scaling argument in Section 5. For $t \gg \tau_q$ we can drop the contributions $z/(t/\tau_q)^{1/4}$ in the last exponential of Eq. (75). The integral over z has been evaluated before in Eq. (53) and the remaining summation and integration involves static terms only

$$\frac{S(q, t)}{S(q)} = 1 - \frac{\Gamma(1/4)}{3\pi} (\gamma_s t)^{3/4} R \quad \text{for } \tau_q \ll t \ll \gamma_s^{-1} \quad (83)$$

with

$$R := \frac{1}{S(q)N} \sum_{n m} \int_{-1}^1 dx \frac{1}{2} (1 - x^2) \exp [iqa(n - m)x + (1 - x^2)q^2 r_{nm}^{1/2}] .$$

This decoupling of static and dynamic contributions also holds for higher orders in the series of Eq. (73). From the derivation it should be clear that $R = 1$, which can be checked explicitly using

$$\frac{1}{2N} \int_{-1}^1 dx (1 - x^2) \frac{\sin^2(kLx/2)}{(kax/2)^2} \xrightarrow{kL \rightarrow \infty} \frac{\pi}{ka} . \quad (84)$$

Neglecting for large times the z dependence in the last exponential of Eq. (75) amounts to replacing in Eq. (70) the reduced cross-correlation $r_{nm}^{\perp 2}(t)$ by its diagonal elements; i.e., for $t \rightarrow \infty$ the time dependence of the structure factor is due to the mean-square segment displacement. (The coherent scattering function of the polymer approaches the incoherent scattering function.) In this approximation the expression in Eq. (70) is reduced to $\pi/qa \cdot \exp(-q^2 r_{nn}^{\perp 2}(t)/4)$ by use of

$$\frac{1}{N} \sum_{nm} e^{iqxa(n-m)} = 2\pi\delta(x). \quad (85)$$

Hence, the decay of the dynamic structure factor is expressed as a stretched exponential as anticipated in Section 5,

$$\frac{S(q, t)}{S(q)} = \exp\left(-\frac{\Gamma(1/4)}{3\pi}(\gamma_s t)^{3/4}\right) \quad (t \gg \tau_q). \quad (86)$$

The stretched exponential tail of the dynamic structure factor is a signature of the bending undulations of the polymer and hence the decay rate γ_s and the crossover time τ_q both depend on the persistence length ℓ_p . In principle the persistence length of a semiflexible polymer can be determined by a comparison of experimental data with Eq. (86). In practice, relative differences in stiffness are easily detected with high accuracy if the diameters of the molecules are known (or are assumed to be identical [33]). In contrast, accurate absolute values are difficult to obtain for several reasons. First, ℓ_p appears in the exponent with a power $1/4$, which makes the method sensitive to experimental error. Second, determining a static quantity by a dynamic method always implies a further model parameter, i.e., we have to specify the friction coefficient. Again in principle, this can be achieved by a measurement of the initial decay rate as suggested in Section 6.2. In practice, however, for the initial decay rate to be determined with some accuracy, $\gamma_i \tau_q$ should not be too small. This implies that one may get problems to find an accurate fit to the tail of the structure factor. Further complications arise from polydispersity, hydrodynamic screening and entanglement effects.

6.4 Entanglement effects

The effects of steric interactions with the surrounding network on the spatio-temporal self-correlations of a single polymer have been discussed in Section 5.4 in the framework of the tube model and the collective modes of an

effective viscoelastic medium. As we already mentioned there, the steric constraints mainly affect the tail of the structure factor. Instead of Eq. (86) we now have

$$\frac{S(q, t)}{S(q)} = \exp \left[-q^2 \delta r_{\perp}^2(\omega_* t) / 4 \right] \quad (87)$$

with $\delta r_{\perp}^2(\omega_*, t)$ from Eq. (66). In principle one should consider the relative contributions of longitudinal and transverse modes to the mean-square displacement separately. The final value of the exponent for long times,

$$2W = \frac{q^2}{3} \langle \mathbf{r}_t^2 + r_t^2 \rangle + \frac{q^2}{3\pi} \left(\frac{k_B T \omega_*^{-1}}{\zeta_{\perp} \ell_p^{1/3}} \right)^{3/4} \quad (88)$$

comprises transverse and longitudinal static fluctuations of the effective medium (first term) and the transverse fluctuations of individual polymer within the tube (second term) according to the equipartition theorem. The long time limit e^{-2W} of $S(q, t)/S(q)$ is known as Lamb-Mössbauer factor in solid state physics. Strictly speaking this notion only applies to a solid body, whereas in the case of a solution one should more accurately speak of an elastic plateau. In reality the plateau seems to be slanted as can be seen from experimental data [77].

Up to now we have concentrated on scattering from a *single* polymer in solution. Although we considered contributions from collective modes to its motion, we still neglected spatio-temporal correlations of different polymers in the scattering function. A scattering experiment that resolves the final slowing down of the decay of the structure factor in time will hardly resolve single polymers in space. For scattering wavelengths much larger than the mesh size, the single polymer scattering function, Eq. (68), is no longer appropriate. The scattering is then described in terms of concentration fluctuations of the collective medium. These also obey a diffusion equation [90, 29, 68] and give rise to a simple exponential decay

$$S_c(q, t) \propto \exp(-q^2 D t) \quad (q \xi_m \ll 1) \quad (89)$$

of the collective dynamic structure factor. Finally, (for even longer times if $L \gg L_e$) one enters the time regime of reptation, where the polymers can wander out of their tubes and the medium exhibits fluid-like behavior.

6.5 Polydispersity and clusters

Apart from steric and hydrodynamic interactions there are other types of “non-ideal” effects that frequently occur in experimental applications. A common problem encountered by experimentalists trying to apply a theory to their measured data is polydispersity of chain length. This subsection contains a short digression to this practically important topic. Conventionally, polydispersity has been analyzed in terms of the moments of the size distribution [52]. However, here we are interested in polydispersity in the limit of large scattering wavelength ($\lambda \gg L$) as the extreme scenario opposite to the situation $\lambda \ll L$ studied above, which is also capable of producing stretched exponential tails in the scattering function. Stretched exponential tails of the structure factor are of course *not* an unambiguous signature of bending modes.

An important example for a strongly polydisperse system is actin, which has been shown to exhibit an approximately exponential length distribution in *in vitro* experiments [47]. The presence of short fragments that diffuse faster than the bending modes of comparable size, certainly affects the dynamic structure factor. However, these effects are negligible, if most of the mass in the solution is contained in long filaments with $L \gg \lambda$. If this is not the case, a theoretical analysis becomes complicated. Beyond the effects discussed so far, we also would have to take into account rotational motion and center of mass diffusion (plus polydispersity) of the polymers, which makes the calculations much more complicated [6, 4, 5, 88]. Moreover, the data analysis becomes ambiguous in the presence of too many fit parameters. In the extreme case of particles which are short enough that we can neglect their internal and rotational dynamics against translational motion (i.e., $L \ll \lambda$), the analysis of polydispersity is rather simple and still interesting enough that we want to mention it here.

Suppose that we have particles of contour length s and diffusion coefficient

$$D_s \simeq \frac{k_B T}{\eta s^{1/\mathcal{D}}} \quad (1 \leq \mathcal{D} \leq d) \quad (90)$$

with a size distribution

$$n_s \propto s^{-\alpha} e^{-s/\Sigma} \quad (91)$$

and a typical size Σ . Our ansatz is general enough to comprise also clusters and aggregates, which occur frequently in the presence of chemical crosslinkers or bad solvents and have been analyzed in the context of gelation [63, 69].

For example we would set $\alpha = 0$, $\mathcal{D} = 1$ for an exponential length distribution of rod-like actin fragments and $\alpha = 5/2$ or $\alpha = 2.2$ for gelation clusters according to mean field theory or percolation theory [89], respectively. In general, the value of α reflects the reaction kinetics of polymerization, aggregation ($\alpha < 2$) or gelation ($\alpha > 2$), while \mathcal{D} characterizes the structures that emanate from this reaction [93].⁹ According to our above assumption of large scattering wavelength we write the scattering function of the solution as

$$S(q, t) = \int_0^\infty ds s^2 n_s \exp(-q^2 D_s t). \quad (92)$$

Introducing the dimensionless length $u := s/\Sigma$ and the characteristic decay rate $\gamma_\Sigma := D_\Sigma q^2$ we rewrite this integral as

$$S(q, t) \propto \int_0^\infty du u^{2-\alpha} \exp\left(-\frac{\gamma_\Sigma t}{u^{1/\mathcal{D}}} - u\right) \quad (93)$$

The special case of $\alpha = 5/2$ and $\mathcal{D} = 1$ can be regarded as a prototype of this kind of integrals. In this case the integral evaluates to a stretched exponential, $S(q, t)/S(q) = e^{-2\sqrt{\gamma_\Sigma t}}$. In other cases of interest, $S(q, t)$ still has a stretched exponential tail (up to logarithmic corrections), as is readily seen from a saddle point approximation,

$$S(q, t) \sim \exp\left(- (1 + \mathcal{D})(\gamma_\Sigma t / \mathcal{D})^{\frac{\mathcal{D}}{1+\mathcal{D}}}\right) \quad (t \rightarrow \infty). \quad (94)$$

Whether the tail is observable in an actual experiment, critically depends on the values of the exponents. For small values of the exponent α , the observed $S(q, t)$ is mostly simple exponential because the stretched exponential tail regime is only reached for very large times $t \gg \gamma_\Sigma^{-1}$.

Compared to the crosslinking of small particles or to the case of small scattering vectors ($q\Sigma \ll 1$), which is included in the foregoing discussion, the situation at large q is more difficult to understand. Additional complications arise in crosslinking of strongly entangled polymer solutions, sometimes referred to as ‘vulcanisation’. In general, there is a trend towards segregation leading to concentration fluctuations [17]. Strongly entangled actin solutions develop super-structures such as bundles and clusters upon crosslinking [91].

⁹The effective viscosity seen by the diffusing particles can in general be different from the pure solvent viscosity η . In particular it may be divergent at the gelation transition as is the typical cluster size Σ [64].

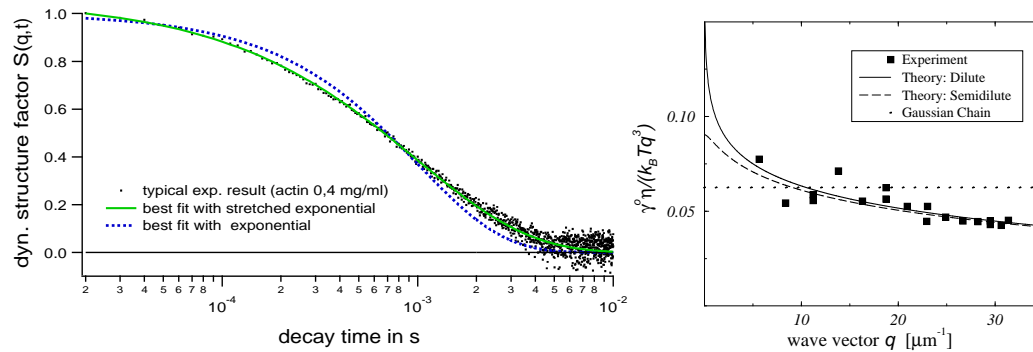


Figure 10: The dynamic structure factor of a semidilute actin solution taken from Reference [33]. Left: The stretched exponential Eq. (86) (on the data) compared to the best single exponential fit. Right: The q –dependence of the initial decay rate, Eq. (80).

The strength of the induced concentration fluctuations increases with the amount of active crosslinkers. If the scattering wavelength λ has been of the order of the mesh size ξ_m prior to crosslinking, there will in general develop regions with $\xi_m < \lambda$ and regions with $\xi_m > \lambda$ upon crosslinking. The scattering signal contains contributions from densely crosslinked clusters or bundles as well as from the rather dilute background medium. The dynamic scattering function of such inhomogeneous networks shows a strong slowing down of the decay as compared to a solution [31]. Only in the ideal case of neatly bound bundles replacing the single filaments, this can be explained according to Eq. (86) by the increased stiffness and diameter of the bundles compared to the single filaments. In general, the long time dynamics can be attributed to the slow motion of the clusters/bundles, while the short time behavior is still due to single filament dynamics within the less dense regions. It is, however, an open question to what extent the results of Section 6.4 can still be applied for a quantitative interpretation. In summary, the complicated scattering signals obtained at large q upon crosslinking of entangled semiflexible polymer networks, although of great experimental and practical interest, are still not very well understood.

6.6 Applications to biopolymers

Light scattering has traditionally been applied as a major tool for the investigation of biopolymers and some of the earlier work has been reviewed

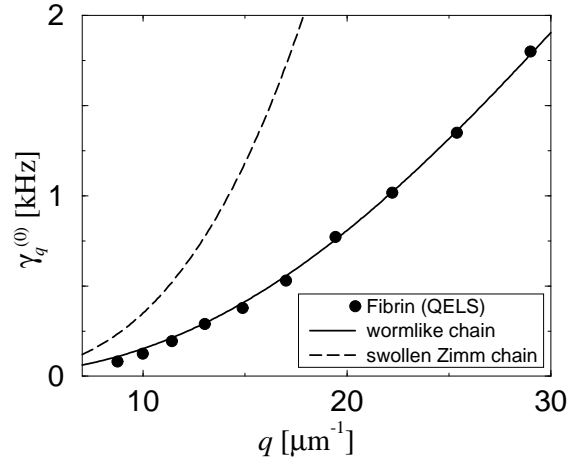


Figure 11: The q –dependence of the initial decay rate. Comparison of the classical result for a swollen Zimm chain [21] with Eq. (80) and quasi-elastic light scattering experiments with the semiflexible biopolymer fibrin [7]. The data were most kindly provided by G. Arcovito.

by Bloomfield [11] and Janmey [45]. As we mentioned in the introduction, biopolymers are important candidates for an application of theories of semiflexible polymers. Especially actin has played a major role as a model semiflexible polymer in some recent investigations [50, 60, 61]. The attempts to determine the persistence length of actin by dynamic light scattering date back to the early 70's [27]. Conventionally, the analysis of scattering data has often been performed in terms of cumulant expansions of the scattering function or decomposition into single exponential contributions. Throughout this contribution we have been emphasizing that sometimes the form of the dynamic scattering function as a whole has to be considered to extract physical information from the data. Our focus has rather been on stretched exponential tails than on expansions or decompositions. However, the theoretical concepts described above are relatively recent developments, and experimental applications are therefore necessarily scarce. The first analysis of experiments in terms of the stretched exponential tail Eq. (86) was performed by Farge and Maggs [22]. They estimated the persistence length of microfilaments from scattering data by Pieckenbrock and Sackmann [74]. The method was refined in later applications [46]. A more detailed analysis of scattering data from actin was performed by Götter *et al.* [33]. Apart from

analyzing the stiffening of actin microfilaments by Eq. (86), these authors used Eq. (80) for the initial decay rate to interpret data taken by Schmidt [81]. In Fig. 10 we reproduce the stretched exponential fit compared to the best single exponential fit (left) and the q -dependence of the initial decay rate (right) from Reference [33]. Though it is not yet clear whether the time resolution of these experiments is sufficient to obtain accurate quantitative results for the lateral diameter of actin filaments from the initial decay rate, the agreement of the data with Eq. (80) is convincing. Very recently, Eq. (80) has successfully been used to analyze dynamic light scattering from fibrin [7] and intermediate filaments such as vimentin and desmin [48, 65, 43], which are more flexible than actin, and therefore better suited for initial decay measurements. The fit of Eq. (80) used to determine the diameter of the biopolymer fibrin has been reproduced from Reference [7] in Fig. 11. These investigations suggest that Eq. (80), though derived in the limit of a weakly bending rod, is in very good agreement with data obtained for rather flexible polymers ($q\ell_p \approx 1$). Measuring the initial slope of the structure factor at various scattering angles compensates partially for the sensitivity of the molecular diameter a to experimental errors, so that the method can be used to determine a by a scattering experiment with $qa \ll 1$. In summary, although there have been some encouraging experimental applications of the theoretical work presented above, the potential of the method for practical applications has not yet been fully explored. In particular, at the time of writing it is still an open question, to what extent Eq. (86) can be used as a quantitative method for determining absolute values of the persistence length, and whether Eq. (87) is able to explain the long time behavior of the scattering function in semidilute solutions.

7 Conclusions

We have reviewed the dynamic structure factor of semiflexible polymers described by the wormlike chain model. The analysis was performed in the limit of long weakly bending rods, i.e., for scattering wavelengths which are relatively short compared to the total contour length and the persistence length of the polymer. We have also introduced the reader to some basic notions of the statistical mechanics of semiflexible polymers and emphasized the difference to the well known Gaussian chain model of flexible polymers. After briefly reviewing some knowledge about the static structure factor of a wormlike chain, we discussed at length the dynamics of a wormlike chain.

The main result is that the dynamic structure factor has a simple exponential short time decay and a stretched exponential tail; cf. Eq. (79) and Eq. (86). In contrast to flexible polymers the stretched exponential tail dominates the time decay for stiff polymers. Very recent experiments with fibrin [7], vimentin [48] and desmin [65, 43] suggest that Eq. (79) may be useful to determine the filament thickness when the scattering wavelength and the persistence length are of about the same size, so that the single exponential initial decay of the structure factor is dominant. We have also discussed modifications of the main results in the presence of steric and hydrodynamic interactions of the polymers in semidilute solutions, when the mesh size is not very small compared to the scattering wavelength, Eq. (87). These more recent extensions of the theory still await experimental verification.

Acknowledgment. This work has been supported by the Deutsche Forschungsgemeinschaft (DFG) through the Sonderforschungsbereich SFB 266. E.F. would like to acknowledge financial support from the DFG through a Heisenberg Fellowship (No. Fr 850/3). We are very grateful for helpful and stimulating discussions with Giuseppe Arcovito, Matthias Fuchs, Bernhard Hinner, Melanie Hohenadl, Paul Janmey, Rudolf Merkel, Erich Sackmann, Jagesh Shah, Jay Tang, David Weitz, and Jan Wilhelm.

A Initial slope from the Smoluchowski equation

Within the Fokker-Planck or Smoluchowski formalism the initial slope of the dynamic structure factor Eq. (68) is given by the expression [21, 1]

$$\gamma^{(0)} \equiv - \left. \frac{d \log S(\mathbf{q}, t)}{dt} \right|_0 = k_B T \frac{\sum_{nm} \langle \mathbf{q} \mathbf{H}(\mathbf{r}_n - \mathbf{r}_m) \mathbf{q} \exp[i\mathbf{q}(\mathbf{r}_n - \mathbf{r}_m)] \rangle}{\sum_{nm} \langle \exp[i\mathbf{q}(\mathbf{r}_n - \mathbf{r}_m)] \rangle} \quad (95)$$

and is in this context directly related to the *frequency matrix* [1]. It is solely dependent on the mobility matrix \mathbf{H} and on the static structure of the polymer. The potential responsible for the conformational properties does not enter explicitly. This can be understood as a consequence of the time scale separation between the stochastic forces and the Brownian dynamics. The fastest motions of a system of Brownian particles are the solvent driven fluctuations around the equilibrium conformation, where the restoring forces from any well behaved conformational potential vanish. These give rise to the initial decay of the dynamic scattering function. In principle, as we have explained in Section 5, the rigid constraint present in the wormlike chain model has to be introduced into the mobility matrix. This has easily been achieved in real space, Eq. (29), but there is no simple way to introduce the rigid constraint into (three dimensional) Fourier space. However, by the following argument we can estimate (and correct for) the error in the calculation of the initial decay rate due to neglecting the rigid constraint. With the Oseen tensor of Eq. (28) excursions transverse to the contour encounter a friction which is twice the friction in the longitudinal direction. This is a consequence of the more effective hydrodynamic backflow interaction along the contour than transverse to the contour. For the same reason the transverse friction coefficient of a rod is two times its longitudinal friction. With the rigid constraint present, however, the motion along the hydrodynamic ‘easy axis’ (the molecule axis) is completely suppressed for a sufficiently long rod in the weakly bending rod approximation, as seen by the opposite sign of the projector in Eq. (29). On the level of counting degrees of freedom (two transverse and one longitudinal) we can thus account for the rigid constraint by dividing by a factor of two the average mobility of the monomers calculated by use of Eq. (28) instead of Eq. (29). To estimate the effect of hydrodynamic screening through possible surrounding network structures we also introduce an infrared cutoff ξ_h for the range of the hydrodynamic interactions as in Eq. (30), so that the appropriate mobility matrix for the

calculation of the initial slope reads

$$\mathbf{H}(\mathbf{r}) = \frac{e^{-r/\xi_h}}{16\pi\eta r} \left(\mathbf{1} + \frac{\mathbf{r} \otimes \mathbf{r}}{r^2} \right), \quad (96)$$

which we represent as a Fourier integral

$$\mathbf{H}(\mathbf{r}_n - \mathbf{r}_m) = \frac{1}{2\eta} \int \frac{d^3 p}{(2\pi)^3} \frac{1}{p^2 + \xi_h^{-2}} \left(\mathbf{1} - \frac{\mathbf{p} \otimes \mathbf{p}}{p^2} \right) \exp[i\mathbf{p}(\mathbf{r}_n - \mathbf{r}_m)]. \quad (97)$$

We thus arrive at the following expression for $\gamma^{(0)}$,

$$\gamma^{(0)} = \frac{k_B T}{2\eta S(\mathbf{q})} \int \frac{d^3 p}{(2\pi)^3} \left(\frac{q^2}{p^2 + \xi_h^{-2}} - \frac{(\mathbf{q}\mathbf{p})^2}{p^2(p^2 + \xi_h^{-2})} \right) S(\mathbf{p} + \mathbf{q}), \quad (98)$$

which we may rewrite in the form

$$\frac{k_B T}{2\eta} \int \frac{d^3 p S(\mathbf{p})}{(2\pi)^3 S(\mathbf{q})} \left(\frac{q^2}{(\mathbf{p} - \mathbf{q})^2 + \xi_h^{-2}} - \frac{(\mathbf{q}(\mathbf{p} - \mathbf{q}))^2}{(\mathbf{p} - \mathbf{q})^2((\mathbf{p} - \mathbf{q})^2 + \xi_h^{-2})} \right), \quad (99)$$

due to the translational invariance of the p -integral, which extends over the whole of p -space. Integrating out the angle between \mathbf{q} and \mathbf{p} we find

$$\begin{aligned} \gamma^{(0)} = & \frac{k_B T}{4\eta} \xi_h^2 \int \frac{dp p^2}{(2\pi)^2} \frac{S(p)}{S(q)} \left(\frac{(p^2 - q^2)^2}{2pq} \log \left| \frac{p - q}{p + q} \right| \right. \\ & \left. + \frac{(p^2 + \xi_h^{-2} - q^2)^2 + 4\xi_h^{-2} q^2}{4pq} \log \frac{(p + q)^2 + \xi_h^{-2}}{(p - q)^2 + \xi_h^{-2}} - \frac{1}{\xi_h^2} \right). \end{aligned} \quad (100)$$

The remaining integral is divergent at the upper bound by virtue of the singular hydrodynamics of the rod, which enters through the static structure factor $S(p)$. As a consequence, the main contributions come from short length scales, which justifies the rod approximation $S(q) \propto q^{-1}$ and forbids – even for a rather flexible polymers – the fractal approximation $S(q) \propto q^{-1/\nu}$ of Eq. (20). As a cutoff for the integral we use the inverse lateral diameter of the molecule $1/a$ and expand the rather lengthy result to leading order in qa and to zeroth order in the screening wave vector ξ_h^{-1} to obtain the expression quoted above,

$$\gamma^{(0)} = \frac{k_B T q^3}{6\pi^2 \eta} \left(\frac{5}{6} - \ln qa \right). \quad (101)$$

More complicated expressions, e.g. the one used for the dashed line in Figs. 9 and 10, result if higher orders of ξ_h^{-1} are not discarded [56].

B Glossary of symbols

a	lateral diameter of the polymer
$D_{t,l}$	diffusion coefficient for transverse/longitudinal collective modes
\mathbf{f}^\perp	Gaussian random force per length
f_c	critical force for buckling
$G(r; L)$	radial distribution function
$\gamma^{(0)}$	initial decay rate (including prefactors)
γ_i	characteristic rate for the initial decay
γ_s	characteristic rate for the stretched exponential decay
Γ	(generalized, incomplete) Γ -function
$\mathbf{H}(\mathbf{r})$	Oseen tensor
$\mathbf{H}_\perp(\mathbf{r})$	transverse projection of the Oseen tensor
κ	bending modulus
K	osmotic compression modulus
k_B	Boltzmann's constant
L	contour length,
L_e	deflection length, entanglement length
ℓ_p	persistence length
λ	scattering wavelength
Λ	cutoff wave number for the effective medium
μ	shear modulus
n, m	indices for the point scatterers along the chain
N	number of point scatterers along the chain
\mathbf{q}	scattering wave vector
$\mathbf{r}(s)$	coordinates of a contour element s
$\mathbf{r}_\perp(s)$	coordinates of contour element s transverse to the average axis
$r_\parallel(s) \equiv s$	coordinate of a contour element s along the average axis
$\delta r_\perp^2(t)$	free mean-square segment displacement
$\delta r_\perp^2(\sigma, t)$	confined mean-square segment displacement
\mathcal{R}^2	mean-square end-to-end distance
\mathcal{R}_g	radius of gyration
s	contour parameter, chemical distance from the end
$S(q)$	static structure factor of a single chain
$S(q, t)$	coherent dynamic structure factor of a single chain
$S_c(q, t)$	collective dynamic structure factor of a solution
σ	force coefficient of the tube potential
t	time
\mathbf{t}	tangent vector

τ_n	mode relaxation time for a free chain
τ_n^e	mode relaxation time for a confined chain
τ_0^e	saturation time for undulations of a confined chain
τ_l	characteristic relaxation time for a transverse excitation of wavelength l
τ_q	crossover time between initial decay and tail regime
T	absolute temperature
$\omega_e^{t,l}$	characteristic relaxation rate of transverse/longitudinal collective modes
ω_*	effective crossover rate from collective modes to single polymer modes
ξ_h	hydrodynamic screening length
ξ_m	mesh size
ζ_{\perp}	friction coefficient per length for transverse contour undulations
ζ	friction coefficient per volume of the effective medium

References

- [1] Akcasu, A. Z. (1993) Dynamic scattering from multicomponent polymer mixtures in solution and in bulk. In *Dynamic Light Scattering: The method and some of its applications*, edited by Brown, W. Clarendon Press, Oxford.
- [2] Akcasu, A. Z., Benmouna, M., and Han, C. C. (1980) *Polymer* **21**, 866.
- [3] Amblard, F., Maggs, A. C., Yurke, B., Pargellis, A. N., and Leibler, S. (1996) *Phys. Rev. Lett.* **77**, 4470.
- [4] Aragón, S. R. (1987) *Macromol.* **20**, 370.
- [5] Aragón, S. R. (1991) *Macromol.* **24**, 3451.
- [6] Aragón, S. R. and Pecora, R. (1985) *Macromol.* **18**, 1868.
- [7] Arcovito, G., Bassi, F., Despirito, M., Distasio, E., and Sabetta, M. (1997) *Biophysical Chemistry* **67**, 287.
- [8] Benoit, H. and Doty, P. M. (1953) *J. Chem. Phys.* **87**, 958.
- [9] Berne, B. J. and Pecora, R. (1976) *Dynamic Light Scattering*. J. Wiley, New York.
- [10] Bhattacharjee, J. K., Thirumalai, D., and Bryngelson, J. D. 1997 Distribution Function of the End-to-End Distance of Semiflexible Polymers. cond-mat/9709345.
- [11] Bloomfield, V. A. (1986) Biological Applications. In *Dynamic Light Scattering: applications of photon correlation spectroscopy*, edited by Pecora, R. Plenum Press, New York.
- [12] Brelford, G. and Krigbaum, W. (1991) Experimental evaluation of the persistence length for mesogenic polymers. In *Liquid crystallinity in polymers*, edited by Ciferri, A., VCH Publishers, Inc., New York.
- [13] Brown, W., editor (1993) *Dynamic Light Scattering: The method and some of its applications*, Oxford, Clarendon Press.

- [14] Brûlet, A., Boué, F., and Cotton, J. P. (1996) *J. Phys. II (Paris)* **6**, 885.
- [15] Caspi, A., Elbaum, M., Granek, R., Lachish, A., and Zbaida, D. (1998) *Phys. Rev. Lett.* **80**, 1106.
- [16] Daniels, H. E. (1952) *Proc. Roy. Soc. Edinburgh* **63A**, 290.
- [17] de Gennes, P. G. (1979) *Scaling Concepts in Polymer Physics*. Cornell University Press, Ithaca and London.
- [18] de Gennes, P.-G. (1981) *J. Phys. (Paris)* **42**, 735.
- [19] des Cloizeaux, J. (1973) *Macromol.* **6**, 403.
- [20] Doi, M. (1996) *Introduction to Polymer Physics*. Clarendon Press, Oxford.
- [21] Doi, M. and Edwards, S. F. (1986) *The Theory of Polymer Dynamics*. Clarendon Press, Oxford.
- [22] Farge, E. and Maggs, A. C. (1993) *Macromol.* **26**, 5041.
- [23] Fisher, M. E. (1963) *Am. J. of Phys.* **32**, 343.
- [24] Frey, E., Kroy, K., and Wilhelm, J. (1998) Viscoelasticity of Biopolymer Networks and Statistical Mechanics of Semiflexible Polymers. In *Molecular Biophysics of the Cytoskeleton*, edited by Malhotra, S. and Tuszynski, J. A. Jai Press.
- [25] Frey, E., Kroy, K., Wilhelm, J., and Sackmann, E. (1998) Statistical Mechanics of Semiflexible Polymers: Theory and Experiment. In *Dynamical Networks in Physics and Biology*, edited by Forgacs, G. and Beysens, D. Springer Verlag, Berlin.
- [26] Frey, E. and Nelson, D. R. (1991) *J. Phys. I France* **1**, 1715.
- [27] Fujime, S. (1970) *J. Phys. Soc. Jap.* **29**, 751.
- [28] Fujime, S. and Maeda, T. (1985) *Macromol.* **18**, 191.

- [29] Geissler, E. (1993) Dynamic light scattering from polymer gels. In *Dynamic Light Scattering. The method and some applications*, edited by Brown, W., Clarendon, Oxford.
- [30] Glatter, O. and Kratky, O. (1982) *Small angle X-ray scattering*. Academic Press, London.
- [31] Goldmann, W. H. et al. (1997) *Eur. J. Biochem* **250**, 447.
- [32] Goldstein, R. E. and Langer, S. A. (1995) *Phys. Rev. Lett.* **75**, 1094.
- [33] Götter, R., Kroy, K., Frey, E., Bärmann, M., and Sackmann, E. (1996) *Macromol.* **29**, 30.
- [34] Granek, R. (1997) *J. Phys. II France* **7**, 1761.
- [35] Grayce, C. (1993) *J. Chem. Phys.* **98**, 9916.
- [36] Harnau, L., Winkler, R. G., and Reineker, P. (1995) *J. Chem. Phys.* **102**, 7750.
- [37] Harnau, L., Winkler, R. G., and Reineker, P. (1996) *J. Chem. Phys.* **140**, 6355.
- [38] Harnau, L., Winkler, R. G., and Reineker, P. (1997) *J. Chem. Phys.* **106**, 2469.
- [39] Harris, R. A. and Hearst, J. E. (1966) *J. Chem. Phys.* **44**, 2595.
- [40] Hermans, J. J. and Ullman, R. (1952) *Physica* **44**, 2595.
- [41] Hickl, P., Ballauff, M., Scherf, U., Müllen, K., and Lindner, P. (1997) *Macromol.* **30**, 273.
- [42] Higgins, J. S. and Benoit, H. C. (1994) *Polymers and Neutron Scattering*. Neutron Scattering in Condensed Matter. Clarendon Press, Oxford.
- [43] Hohenadl, M. (1998) Untersuchung der mechanischen Eigenschaften von Desminfilamenten mit Hilfe dynamischer Lichtstreuung. Master's thesis, Technische Universität München.

- [44] Janmey, P. (1995) Cell Membranes and the Cytoskeleton. In *Structure and Dynamics of Membranes*, edited by Lipowsky, R. and Sackmann, E., volume 1A of *Handbook of biological physics*, North Holland, Amsterdam.
- [45] Janmey, P. A. (1993) Application of dynamic light scattering in biological systems. In *Dynamic light scattering*, edited by Brown, W., Clarendon Press, Oxford.
- [46] Janmey, P. A. et al. (1994) *J. Biol. Chem.* **269**, 32503.
- [47] Janmey, P. A., Peetermans, J., Zaner, K. S., Stossel, T. P., and Tanaka, T. (1986) *J. Biol. Chem.* **261**, 8357.
- [48] Janmey, P. A. and Shah, J. (1998). Private communication.
- [49] Käs, J., Strey, H., and Sackmann, E. (1994) *Nature* **368**, 226.
- [50] Käs, J. et al. (1996) *Biophys. J.* **70**, 609.
- [51] Kholodenko, A. L. (1993) *Macromol.* **26**, 4179.
- [52] Koppel, D. E. (1972) *J. Chem. Phys.* **57**, 4814.
- [53] Koyama, R. (1973) *J. Phys. Soc. Jap.* **34**, 1029.
- [54] Kratky, O. and Porod, G. (1949) *Rec. Trav. Chim.* **68**, 1106.
- [55] Kroy, K. and Frey, E. (1996) *Phys. Rev. Lett.* **77**, 306.
- [56] Kroy, K. and Frey, E. (1997) *Phys. Rev. E* **55**, 3092.
- [57] Kroy, K. and Frey, E. (1998) Viscoelasticity of gels and solutions of semiflexible polymers. unpublished.
- [58] Lagowski, J. B., Noolandi, J., and Nickel, B. (1991) *J. Chem. Phys.* **95**, 1266.
- [59] Lagowski, J. B., Noolandi, J., and Nickel, B. (1992) *J. Chem. Phys.* **96**, 3362.
- [60] MacKintosh, F. and Janmey, P. A. (1997) *Curr. Op. Cell. Biol.* **2**, 350.

-
- [61] Maggs, A. C. (1997) Actin, a model semi-flexible polymer. cond-mat/9704054.
- [62] Marques, C. M. and Fredrickson, G. (1997) *J. Phys. II France* **7**, 1805.
- [63] Martin, J. E. and Adolf, D. (1991) *Ann. Rev. Phys. Chem.* **42**, 311.
- [64] Martin, J. E. and Wilcoxon, J. P. (1988) *Phys. Rev. Lett.* **61**, 373.
- [65] Merkel, R. (1998). Private communication.
- [66] Muthukumar, M. and F., E. S. (1983) *Macromol.* **16**, 1475.
- [67] Neugebauer, T. (1943) *Ann. Phys. (Leipzig)* **42**, 509.
- [68] Nicolai, T. and Brown, W. (1996) Scattering from concentrated polymer solutions. In *Light Scattering. Principles and Development*, edited by Brown, W., Clarendon Press, Oxford.
- [69] Nicolai, T., Durand, D., and Gimel, J.-C. (1996) Scattering properties and modelling of aggregating and gelling systems. In *Light Scattering. Principles and Development*, edited by Brown, W., Clarendon Press, Oxford.
- [70] Norisuye, T., Murakama, H., and Fujita, H. (1978) *Macromol.* **11**, 966.
- [71] Odijk, T. (1983) *Macromol.* **16**, 1340.
- [72] Pedersen, J. S. and Schurtenberger, P. (1996) *Macromol.* **29**, 7602.
- [73] Pezron, I., Djabourov, M., and Leblond, J. *Polymers* **32**, 3201.
- [74] Pieckenbrock, T. and Sackmann, E. (1992) *Biopolymers* **32**, 1471.
- [75] Ronca, G. (1983) *J. Chem. Phys.* **79**, 1031.
- [76] Rouse, P. E. (1953) *J. Chem. Phys.* **21**, 1272.
- [77] Sackmann, E. Unpublished data. Private communication.
- [78] Sackmann, E. (1994) *Macromol. Chem. Phys.* **195**, 7.
- [79] Saitô, N., Takahashi, K., and Yunoki, Y. (1967) *J. Phys. Soc. Jap.* **22**, 219.

- [80] Schaefer, D. W. and Han, C. C. (1986) Quasielastic Light Scattering from Dilute and Semidilute Polymer Solution. In *Dynamic Light Scattering: applications of photon correlation spectroscopy*, edited by Pecora, R., Plenum Press, New York.
- [81] Schmidt, C. F. (1988) *Dynamik und Struktur polymerer Aktin-Netzwerke und ihre Wechselwirkung mit Modellmembranen*. PhD thesis, Technische Universität München.
- [82] Schmitz, K. S. (1990) *Dynamic Light Scattering by Macromolecules*. Academic Press, Boston.
- [83] Seifert, U., Wintz, W., and Nelson, P. (1996) *Phys. Rev. Lett.* **77**, 5389.
- [84] Sharp, P. and Bloomfield, V. A. (1953) *Biopolymers* **6**, 1201.
- [85] Smith, S. B., Finzi, L., and Bustamante, C. (1992) *Science* **258**, 1122.
- [86] Soda, K. (1973) *J. Phys. Soc. Jpn.* **35**, 866.
- [87] Soda, K. (1984) *Macromol.* **17**, 2365.
- [88] Song, L., Kim, U. S., Wilcoxon, J., and Schurr, J. M. (1991) *Biopolymers* **31**, 547.
- [89] Stauffer, D., Coniglio, A., and Adam, M. (1982) *Adv. Pol. Sci.* **44**, 103.
- [90] Tanaka, T., Hocker, L. O., and Benedek, G. B. (1973) *J. Chem. Phys.* **59**, 5151.
- [91] Tempel, M., Isenberg, G., and Sackmann, E. (1996) *Phys. Rev. E* **54**, 1802.
- [92] Thompson, C. J. (1972) *One-Dimensional Models — Short Range Forces*, volume 1 of *Phase Transitions and Critical Phenomena*, chapter 5. Academic Press, London.
- [93] Van Dongen, G. P. I. and Ernst, M. H. (1985) *Phys. Rev. Lett.* **54**, 1396.

-
- [94] Weitz, D. A. and Pine, D. J. (1993) Diffusing-wave spectroscopy. In *Dynamic Light Scattering. The method and some applications*, edited by Brown, Clarendon, Oxford.
- [95] Wiggins, C. H., Riveline, D. X., Ott, A., and Goldstein, R. E. (1998) *Biophys. J.* **74**, 1043.
- [96] Wilhelm, J. and Frey, E. (1996) *Phys. Rev. Lett.* **77**, 2581.
- [97] Winkler, R. G., Reineker, P., and Harnau, L. (1994) *J. Chem. Phys.* **101**, 8119.
- [98] Yamakawa, H. (1971) *Modern Theory of Polymer Solutions*. Harper & Row, New York.
- [99] Yamakawa, H. and Fujii, M. (1974) *Macromol.* **7**, 649.
- [100] Yoshizaki, T. and Yamakawa, H. (1980) *Macromol.* **13**, 1518.
- [101] Yoshizaki, T. and Yamakawa, H. (1997) *J. Chem. Phys.* **106**, 2828.
- [102] Zimm, B. H. (1956) *J. Chem. Phys.* **24**, 269.